Journal of Experimental Botany, Vol. 71, No. 3 pp. 934–950, 2020
doi:10.1093/jxb/erz475 Advance Access Publication October 23, 2019

RESEARCH PAPER

miR156-targeted *SPL10* controls Arabidopsis root meristem activity and root-derived *de novo* shoot regeneration via cytokinin responses

Carlos Hernán Barrera-Rojas[1,2], Gabriel Henrique Braga Rocha[1], Laura Polverari[3], Diego Armando Pinheiro-Brito[1], Diego Silva Batista[4], Marcela M. Notini[1], Ana Claudia Ferreira da Cruz[4], Edna Gicela Ortiz Morea[1,2], Sabrina Sabatini[3], Wagner Campos Otoni[4] and Fabio Tebaldi Silveira Nogueira[1,*]

[1] Laboratory of Molecular Genetics of Plant Development, Department of Biological Sciences, Escola Superior de Agricultura 'Luiz de Queiroz', University of Sao Paulo, 13418–900 Piracicaba, Sao Paulo, Brazil
[2] Bioscience Institute, State University of Sao Paulo, Botucatu, Sao Paulo 18618–970, Brazil
[3] Laboratory of Functional Genomics and Proteomics of Model Systems, Dipartimento di Biologia e Biotecnologie, Università La Sapienza, 00185, Rome, Italy
[4] Department of Plant Biology, Plant Tissue Culture Laboratory-BIOAGRO, Federal University of Viçosa, 36570–900 Viçosa, MG, Brazil

* Correspondence: ftsnogue@usp.br

Received 12 September 2019; Editorial decision 1 October 2019; Accepted 1 October 2019

Editor: Rüdiger Simon, Heinrich Heine University, Germany

Abstract

Root growth is modulated by different factors, including phytohormones, transcription factors, and microRNAs (miRNAs). MicroRNA156 and its targets, the *SQUAMOSA PROMOTER BINDING PROTEIN-LIKE* (*SPL*) genes, define an age-dependent pathway that controls several developmental processes, including lateral root emergence. However, it remains unclear whether miR156-regulated *SPL*s control root meristem activity and root-derived *de novo* shoot regeneration. Here, we show that *MIR156* and *SPL* genes have opposing expression patterns during the progression of primary root (PR) growth in Arabidopsis, suggesting that age cues may modulate root development. Plants with high miR156 levels display reduced meristem size, resulting in shorter primary root (PRs). Conversely, plants with reduced miR156 levels show higher meristem activity. Importantly, loss of function of *SPL10* decreases meristem activity, while *SPL10* de-repression increases it. Meristem activity is regulated by *SPL10* probably through the reduction of cytokinin responses, via the modulation of type-B *ARABIDOPSIS RESPONSE REGULATOR1*(*ARR1*) expression. We also show that *SPL10* de-repression in the PRs abolishes *de novo* shoot regenerative capacity by attenuating cytokinin responses. Our results reveal a cooperative regulation of root meristem activity and root-derived *de novo* shoot regeneration by integrating age cues with cytokinin responses via miR156-targeted *SPL10*.

Keywords: *Arabidopsis thaliana*, *de novo* shoot regeneration, meristem, microRNA156, root, *SPL*s.

Introduction

The functions of the root system (RS) are partially dependent on the root length, which is determined by the number of proliferating cells in the meristem and their final mature size (Zobel, 1986; Beemster and Baskin, 1998). In Arabidopsis, the RS comprises a primary root (PR), lateral roots (LRs) and, eventually, adventitious roots. The Arabidopsis RS has a single embryonic-derived PR, which generally remains active throughout the plant life cycle (Hodge, 2006; Osmont *et al.*, 2007). Root growth is maintained by the root meristem, a sustainable and self-renewable system the activity of which depends upon a number of different factors, including phytohormones, transcription factors, and microRNAs (miRNAs) (Dello Ioio *et al.*, 2008; Takatsuka and Umeda, 2014; Couzigou and Combier, 2016). However, how these different factors are integrated to control meristem size and root growth remains unclear.

Auxin and cytokinin are essential for root growth and development as they control meristem activity and root organogenesis (Dello Ioio *et al.*, 2007, 2008; Di Mambro *et al.*, 2017). In the PR, auxin establishes positional information for cell fate decisions and maintains root meristem activity by promoting cell division. The cell proliferation zone is characterized by intermediate auxin concentrations, whilst low levels of auxin are found in the elongation and differentiation zones along the root longitudinal axis (Burstrom, 1957; Petersson *et al.*, 2009; Jurado *et al.*, 2010). These auxin gradients are partially generated by PIN-FORMED (PIN) auxin-efflux carriers, which funnel auxin efflux between cells (Blilou *et al*, 2005; Vieten *et al*, 2005; Wisniewska *et al*, 2006). *PIN1*, *PIN3*, and *PIN7* have been shown to be essential to control root meristem size (Dello Ioio *et al.*, 2007). On the other hand, cytokinin antagonizes auxin by promoting cell differentiation in roots. Cytokinin controls root meristem size by activating the nucleus-localized type-B ARABIDOPSIS RESPONSE REGULATORS (ARRs) ARR1 and ARR12. Type-B ARRs are GARP transcription factors that control the expression of cytokinin-regulated genes, including type-A *ARR*s such as *ARR5* (Mason *et al.*, 2004). Type-B ARR1 and the ARR12 repress the expression of the *PIN* genes through the SHY2/IAA3 protein, a repressor of auxin signaling (Dello Ioio *et al.*, 2007; 2008). Thus, cytokinin and auxin antagonistically interact at the transition zone to balance cell differentiation with cell division, which is essential to stabilize meristem size and to ensure continuous root growth (Dello Ioio *et al.*, 2007; 2008). Similar to PR growth, the balance between auxin and cytokinin is critical for LR development. This process initiates with the establishment of LR primordia, regulated by local auxin accumulation in pericycle cells termed 'founder cells', leading to LR organogenesis (Fukaki *et al.*, 2002; De Smet *et al.*, 2007, 2010; Péret *et al.*, 2009; Dastidar *et al.*, 2012). Resembling LR initiation, formation of callus (a mass of growing cells) from PR explants initiates with pericycle cell divisions driven by local auxin maxima in the founder cells (Che *et al.*, 2007; Sugimoto *et al.*, 2010). Competent cells from callus tissue are committed to a shoot or root fate according to the auxin/cytokinin balance. A high cytokinin:auxin ratio directs these cells to undergo shoot formation, while a low ratio induces root differentiation (Skoog and Miller, 1957). Importantly, explants derived from different tissues share the anatomical and molecular determinants of organ-primordia formation with root explants (Sugimoto *et al.*, 2010).

MiRNA-regulated pathways are also fundamental for root growth and patterning (Rubio-Somoza and Weigel, 2011; Couzigou and Combier, 2016). miRNAs are a group of small RNAs (21–24 nt) that modulate gene expression in both animals and plants (Lagos-Quintana *et al.*, 2001; Jones-Rhoades *et al.*, 2006). Several miRNA-regulated pathways affect different root developmental processes. For instance, the miR396/*GROWTH RESPONDING FACTOR* (*GRF*) pathway regulates the transition of root stem cells to transit-amplifying cells (Rodriguez *et al.*, 2015). While the miR164/*NAM*, *ATAF*, *CUC2* (*NAC*) and miR160/*AUXIN RESPONSE FACTOR10* (*ARF10*) pathways are crucial in controlling LR initiation (Mallory *et al.*, 2004; Guo *et al.*, 2005; Wang *et al.*, 2005), the miR167/*ARF6/8* and miR390/*TAS/ARF3/4* pathways act subsequently during emergence and elongation of the LR (Gifford *et al.*, 2008; Marin *et al.*, 2010; Yoon *et al.*, 2010). In addition, the regulation of the class III homeodomain zipper transcription factors by miR166/165 in the root endodermis and stele periphery is crucial in determining xylem cell types in a dosage-dependent manner (Carlsbecker *et al.*, 2010).

MiR156 and its targets, the SQUAMOSA PROMOTER-BINDING PROTEIN-LIKE (SPL) family of transcription factors (Wu and Poethig, 2006; Morea *et al.*, 2016), define an age-dependent pathway that is crucial for several developmental processes (Wu and Poethig, 2006; Wu *et al.*, 2009; Xie *et al.*, 2012; Silva *et al.*, 2014, 2019; Xu *et al.*, 2016). Increasing miR156-targeted *SPL* levels lead to a progressive decline in *de novo* shoot regenerative capacity of aerial tissues (leaves and hypocotyls) as the plant ages (Zhang *et al.*, 2015). Increasing miR156 expression in rice leads to the development of more roots with smaller size (Xie *et al.*, 2012), whereas high expression of miR156 is necessary for adventitious root formation in *Malus xiaojinensis* (Xu *et al.*, 2017). Arabidopsis plants overexpressing *MIR156* genes produce more LRs, while reduced miR156 levels leads to fewer lateral and eventually adventitious roots (Yu *et al.*, 2015; Xu *et al.*, 2016). MiR156-targeted *SPL3*, *SPL9*, and *SPL10* are involved in repressing LR primordium emergence, with *SPL10* playing a dominant role (Yu *et al.*, 2015). These findings suggest an important role of the miR156/*SPL* pathway in controlling root system architecture, yet the mechanisms underlying the functions of miRNA156-targeted *SPL*s in this developmental process are largely unknown. MiR156-targeted *SPL*s may affect shoot meristem size (Wang *et al.*, 2008; Fouracre and Poethig, 2019), but it is unclear if such a regulation is shared with the root meristem. Moreover, it is unknown whether the miR156-controlled network intersects with auxin and cytokinin to modulate root meristem activity and *de novo* shoot regenerative capacity of root explants.

Here, we show that the miR156/*SPL* module has a role in Arabidopsis PR growth by altering root meristem activity

mostly via modulating cytokinin responses. We found that high levels of miR156 reduced root meristem size, whilst low levels of miR156 increased it. Arabidopsis plants expressing a miR156-resistant version of *SPL10* (*rSPL10*) exhibited longer PRs and increased meristem size, while loss-of-function of *SPL10* produced shorter PRs and reduced meristem size. *ARR1*-dependent cytokinin responses were reduced by *SPL10* and it may have unbalanced cell differentiation and cell division rates, thus readjusting meristem size and PR length. These modifications in cytokinin responses also had a negative effect on the *de novo* shoot regenerative capacity of *rSPL10* PRs since they were unable to regenerate shoots and instead generated highly differentiated meristemoid-like structures. Together, our results suggest that the recruitment of age cues via miR156-targeted *SPL*s contributes to modulation of root meristem activity and root-derived shoot regenerative capacity.

Material and methods

Plant material and growth conditions

The *Arabidopsis thaliana* plants used in this study were of the Columbia (Col-0) ecotype. Transgenic plants expressing *p35S::MIR156A*, miR156-sensitive (*pSPL3::sSPL3-GUS*, *pSPL6::sSPL6-GUS*, *pSPL9::sSPL9-GUS*, *pSPL10::sSPL10-GUS*), miR156-resistant (*pSPL3::rSPL3-GUS*, *pSPL6::rSPL6-GUS*, *pSPL9::rSPL9-GUS*, *pSPL10::rSPL10-GUS*, *pSPL9::rSPL9*, *pSPL10::rSPL10*), and the CRISPR/Cas9-derived *spl10-2* have been described previously by Wu and Poethig (2006) and Xu *et al.* (2016). Transgenic plants harboring a target mimic against miR156 (*p35S::MIM156*or *MIM156*) have been described previously by Franco-Zorrilla *et al.* (2007). Arabidopsis plants harboring the *pMIR156A::MIR156A-GUS* and *pMIR156C::MIR156C-GUS* constructs have been described by Yang *et al.* (2013). Plants harboring the reporter constructs *pCYCLINB1;1::GUS*, *pDR5::GFP*, *pPIN1::PIN1-GFP*, and *TCSn::GFP* have been described previously by Ferreira *et al.* (1994) Ulmasov *et al.* (1997), Su and Zhang (2009), and Zürcher *et al.* (2013). Arabidopsis plants harboring the reporter *pARR5::GUS* were obtained by introducing the *pARR5::GUS* construct (D'Agostino *et al.*, 2000) into Col-0 plants using the floral dip method Clough and Bent (1998). At least 10 independent transgenic lines with similar expression patterns were obtained, and one was selected for further use at the T_3 generation. Arabidopsis *arr1-4* plants have been described previously by Dello Ioio *et al.* (2007).

For cultivation of plants, seeds were surface-sterilized with 1.0% bleach for 10 min and washed three times with sterile water. The seeds were then sown on sterile plates containing half-strength Murashige and Skoog (MS) medium (Murashige and Skoog, 1962) supplemented with 1.0% (w/v) sucrose and 0.6% (w/v) phytagar. Seeds were placed at 4 °C for 2 d for stratification. The plates were then placed vertically in a growth chamber under long-day conditions (16/8 h light/dark) at 22 °C.

Root growth assays and meristem size analysis

For root growth analyses, PRs from seedlings at 5, 10, and 15 d post-germination (dpg) were scanned and measured using the ImageJ software (https://imagej.nih.gov/ij/). For root growth rate (RGR), seedlings at 5 dpg were transferred to plates containing MS medium supplemented with 0.1 μM or 1.0 μM 6-benzyladenine (6-BA) and maintained for either 4 d or 5 d in a growth chamber. After the treatment with 6-BA, RGR was measured as the increment in the root length compared with that at the beginning of the treatment (n=45 seedlings) using ImageJ. Analyses of the meristem size were performed under a light microscope by counting the cortex cell number on a file of cells extended from the quiescent center to the transition zone (Dello Ioio *et al.*, 2007, 2008). At least 10 seedlings were evaluated.

Root-derived de novo shoot organogenesis

Roots from 7- or 10-dpg seedlings of Col-0 were excised below the hypocotyl and transferred to a callus-induction medium (CIM) (Qiao *et al.*, 2012) composed of B5 basal medium (Gamborg *et al.*, 1968) supplemented with 0.5 g l^{-1} 2-(N-morpholino)-ethanesulfonic acid (MES), 2.2 μM 2,4-dichlorophenoxyacetic acid (2,4-D), 0.2 μM kinetin, 20 g l^{-1} glucose, and 7.0 g l^{-1} agar, with pH adjusted to 5.75. After 4 d in the CIM, the explants were transferred to a shoot-induction medium (SIM) (Qiao *et al.*, 2012) composed of MS medium supplemented with 2.5, 5.0, or 10.0 μM isopentenyladenine (2-iP), 0.9 μM indole-3-acetic acid (IAA), 10 g l^{-1} sucrose and 7.0 g l^{-1} agar, pH 5.75. The explants were then incubated at 25 °C under long-day conditions. The regenerative capacity was evaluated by counting the number of regenerated shoots from root explants derived from the 7- and 10-dpg seedlings. All experiments were repeated three times with similar results.

Histological analysis and SEM

Samples of root explants were fixed in Karnovsky solution (Karnovsky, 1965), dehydrated in an increasing ethanol series (10–100%), and subsequently infiltrated into synthetic resin using a HistoResin Embedding Kit (Leica) according to the manufacturer's protocol. Tissue sections were obtained using a rotary microtome and stained with Toluidine Blue 0.05% (Sakai, 1973). Permanent slides were mounted with synthetic resin (Entellan®, Merck). For SEM, samples were fixed, mounted, and examined as described by Bharathan *et al.* (2002).

RNA extraction, RT-PCR, and qRT–PCR

Total RNA was isolated using Trizol reagent (ThermoFisher) according to the manufacturer's instructions, then treated with DNase I (Invitrogen). Samples of the RNA (2 μg) were then used to generate first-strand cDNA. For mature miRNA, a stem-loop RT primer was designed to hybridize the mature miR156 molecule, and then reverse-transcribed in a pulsed RT reaction, according to Varkonyi-Gasic *et al.* (2007). The RT product was amplified using a miRNA-specific forward primer and the universal reverse primer. Reactions for RT-PCR and qRT-PCR were done as described by Silva *et al.* (2014). qRT-PCR reactions were performed in a StepOnePlus™ real-time PCR system (ThermoFisher). Each sample was comprised of PRs from at least 50 seedlings. For RT-PCR expression analyses, three biological samples were used. Three biological samples with two technical replicates each were used in the qRT-PCR analyses. *ACTIN-2* was used as the reference gene (Yu *et al.*, 2015): we analysed *ACTIN-2* expression levels in order to compare with other potential reference genes (Supplementary Fig. S1Aat *JXB* online; Czechowski *et al.*, 2005). Expression levels were then calculated relative to *ACTIN-2* using the $2^{-\Delta\Delta CT}$ method (Livak and Schmittgen, 2001). The primers used are listed in Supplementary Table S1.

GUS staining and GFP analysis

The GUS (ß-glucoronidase) staining protocol followed that of Senecoff *et al.* (1996). GFP images were obtained with the Zeiss Epifluorescence imager D2 using a specific filter for GFP analysis. For each line and treatment, at least 10 seedlings were analysed.

Accession numbers

SPL2 (AT5G43270), *SPL3* (AT2G33810), *SPL4* (AT1G53160), *SPL5* (AT3G15270), *SPL6* (AT1G69170), *SPL9* (AT2G42200), *SPL10* (AT1G27370), *SPL11* (AT1G27360), *SPL13* (AT5G50570), *SPL15* (AT3G57920), *MIR156A* (AT2G25095), *MIR156C* (AT4G31877), *PIN1* (AT1G73590), *PIN3* (AT1G70940), *PIN7* (AT1G23080), *ARR1* (AT3G16857), *ARR12*(AT2G25180), *SHY2* (AT1G04240), *CYCLINB1;1* (AT4G37490), and *ACTIN-2* (AT3G18780).

Results

MIR156 *expression decreases with time during PR growth*

The Arabidopsis genome contains eight *MIR156* genes and their expression patterns have been extensively studied in leaves (Yang *et al.*, 2013; Xu *et al.*, 2018). In the aerial tissues, *MIR156A and MIR156C* are the major sources of mature miR156 and their expression declines as the plant ages; however, the situation in roots is unclear (Yang *et al.*, 2013;Yu *et al.*, 2015; Xu *et al.*, 2018). We therefore examined the expression of *MIR156A* and *MIR156C* in roots at 5-, 10-, and 15-dpg. First, we used GUS staining to evaluate gene expression in transgenic plants separately harboring the *pMIR156A::MIR156A-GUS* (*MIR156A-GUS*) and *pMIR156C::MIR156C-GUS* (*MIR156C-GUS*) constructs previously described by Yang *et al.* (2013). Expression of *MIR156A* (Fig. 1A–D) and *MIR156C* (Fig. 1F–I) was detected in all zones of the PR in seedlings at 5-, 10-, and 15-dpg; importantly, GUS staining decreased over time for both *MIR156A-GUS* (Fig. 1A) and *MIR156C-GUS* (Fig. 1F). To confirm these temporal expression patterns, we examined the levels of *MIR156A* and *MIR156C* precursor transcripts in roots of Col-0 using qRT-PCR and found that both also decreased over time (Fig. 1E, J). These results indicated that *MIR156A* and *MIR156C* may also have roles in controlling PR growth during plant development.

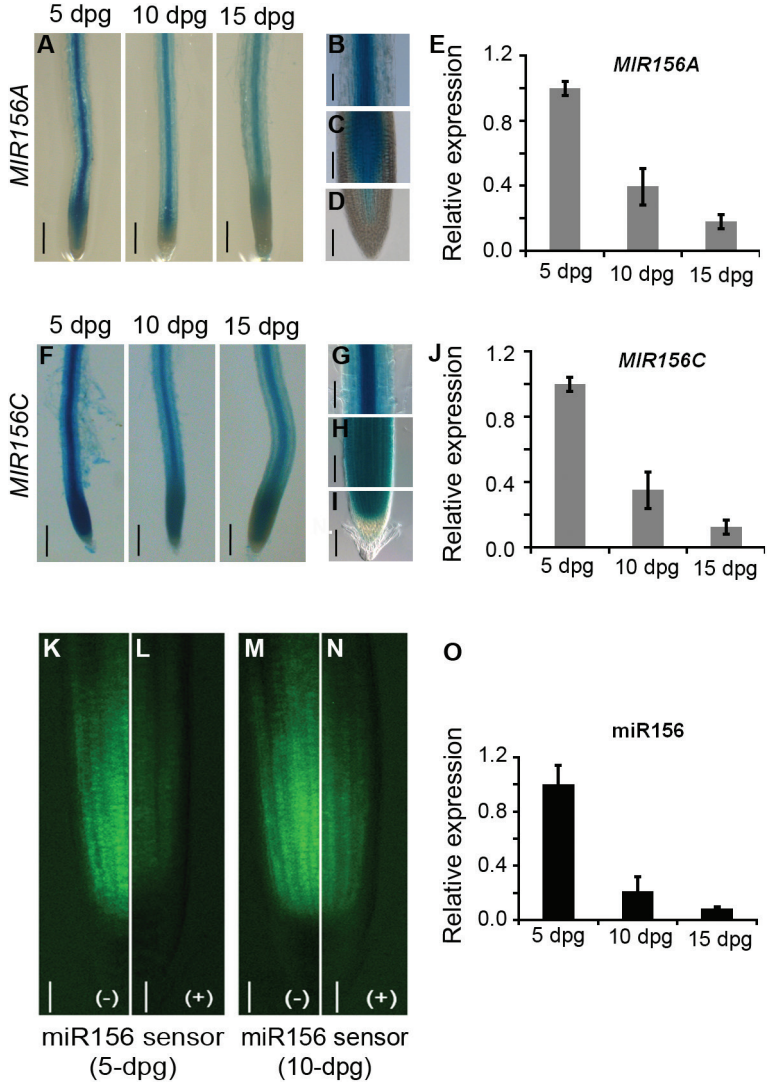

Fig. 1. *MIR156* is dynamically expressed during the progression of root growth in Arabidopsis. (A–D) Expression patterns as indicated by GUS staining of *MIR156A* in primary roots (PRs) of seedlings at (A) 5, 10, and 15 d post-germination (dpg). *MIR156A-GUS* is detected in (B) the maturation, (C) elongation, and (D) meristematic zones of roots at 10 dpg. (E) Expression of *MIR156A* in roots of wild-type Col-0 seedlings as determined by qRT-PCR. Expression is relative to that of roots at 5 dpg, the value of which was set to 1. (F–I) Expression patterns as indicated by GUS staining of *MIR156C* in PRs of seedlings at (F) 5-, 10-, and 15-dpg. *MIR156C–GUS* is detected in the (G) maturation, (H) elongation, and (I) meristematic zones of roots at 10 dpg. (J) Expression of *MIR156C* in roots of wild-type Col-0 seedlings as determined by qRT-PCR. Expression is relative to that of roots at 5 dpg, the value of which was set to 1. (K–N) Microscope images of epifluorescence from the root tips of seedlings expressing miR156-GFP. (K, L) Seedlings at 5 dpg either (J) without or (K) with the miR156 target site (indicated by – and +, respectively), and (M, N) seedlings at 10 dpg either (M) without or (N) with the target site. (O) Expression of mature miR156 in roots of wild-type Col-0 seedlings as determined by qRT-PCR. Expression is relative to that of roots at 5 dpg, the value of which was set to 1. Scale bars are 250 μm (A, F), 100 μm (B–D, G–I), and 50 μm in (K–N). The images shown are representative individuals of at least five seedlings of each genotype. Data in (E, J, O) are means (±SE) of three biological samples. (This figure is available in colour at *JXB* online.)

Next, we used transgenic plants harboring a GFP-based miR156 sensor (+) and plants without the miR156 sensor (–) (Nodine and Bartel, 2010) to evaluate the activity of mature miR156 in PRs. Compared with the –miR156 sensor, the +miR156 sensor had a reduced GFP signal throughout the meristematic and transition zones, and it increased in PR at 10-dpg compared with 5-dpg (Fig. 1K–N). Similarly, mature miR156 transcript levels decreased during PR growth (Fig. 1O). Together, these results indicated that miR156 was localized and active throughout the meristematic and transition zones, and that its levels and activity decreased during the progression of PR growth.

miR156-dependent regulation is required for the spatiotemporal expression of SPL*s in the PR*

MIR156 expression decreased in the PRs over time, and therefore an opposing expression pattern of *SPL*s would be expected. Ten *SPL* genes are post-transcriptionally regulated by miR156 in Arabidopsis and they are grouped into four clades, with *SPL3*, *SPL6*, *SPL9*, and *SPL10* being their representative members (Guo *et al.*, 2008). To determine whether *SPL*s had roles in modulating PR growth, we examined the spatiotemporal expression patterns of these representative members and the contribution of miR156 to these patterns. We compared transgenic plants expressing either a miR156-sensitive (*pSPL::sSPL*) or a miR156-resistant (*pSPL::rSPL*) version of the fusion protein tagged with GUS under the control of their own promoters (Xu *et al.*, 2016). The resistant versions are characterized by the insertion of silent mutations into the miR156 response element that abolish the interaction of mature miR156 with *SPL*s, and are hereafter referred to as *rSPL3-GUS*, *rSPL6*-GUS, *rSPL9*, and *rSPL10* (Li *et al.*, 2012; Xu *et al.*, 2016).

GUS staining was not detected in the PR of the miR156-sensitive version of the *SPL3* reporter (*sSPL3-GUS*) at 5, 10, or 15 dpg (Supplementary Fig. S1B–D); however, staining was observed in the miR156-resistant version (*rSPL3-GUS*), mostly in the transition and elongation zones, and (as expected) it increased from 5dpg to 15 dpg (Supplementary Fig. S1E–G). Expression of *rSPL3-GUS* was not observed in the meristematic zone (Supplementary Fig. S1E, F). qRT-PCR data confirmed that *SPL3* transcript levels increased in the PR of wild-type Col-0 plants from 5dpg to 15 dpg (Supplementary Fig. S1H). GUS staining in the miR156-sensitive version of the *SPL6* reporter (*sSPL6-GUS*) was not detected at any developmental time-point (Supplementary Fig. S2A–C); however, in the resistant version (*rSPL6-GUS*) it was detected at low but consistent levels in pericycle cells of the meristematic and transition zones of the PR at 10 and 15 dpg (Supplementary Fig. S2 D–F). Moreover, qRT-PCR data showed no changes in transcript levels of *SPL6* over time during the growth of the PR (Supplementary Fig. S2 G).

GUS staining in the miR156-sensitive version of *SPL9* reporter (*sSPL9-GUS*) was observed in the stele of the meristematic, transition, and elongation zones (Fig. 2A–D, I). In the resistant version, *rSPL9-GUS* was strongly expressed throughout the PR, as well as in LRs (Fig. 2E–H, J). Interestingly, *SPL9* transcript levels peaked at 10 dpg and were reduced at 15 dpg (Fig. 2O), as was also observed by GUS staining in both the miR156-sensitive and -resistant versions at 15 dpg (Fig. 2A, E), suggesting the existence of a miR156-independent mechanism of *SPL9* regulation at this developmental stage. GUS staining in the sensitive version of the *SPL10* reporter (*sSPL10-GUS*) was observed specifically in the meristematic zone of PRs at 10 and 15 dpg (Fig. 2K), but not in LRs (Fig. 2M). On the other hand, the resistant version, *rSPL10-GUS*, was observed in the meristematic and transition zones and LRs at all developmental times, and it increased over time (Fig. 2L, N). qRT-PCR data showed that transcript levels of *SPL10* increased throughout root growth, confirming the data observed by GUS staining (Fig. 2P). Thus, the data indicated that the representative members of the *SPL* clades displayed distinct expression patterns during the progression of PR growth, and their regulation in the PR was mostly miR156-dependent. *SPL10* expression in the meristematic and transition zones suggested it had a possible role in the maintenance of PR meristem activity, and hence in growth.

*Disruption of the miR156/*SPL *balance affects the size of the root meristem and PR growth*

It has been shown that emergence of LRs in Arabidopsis is regulated by miR156-targeted *SPL3*, *SPL9*, and *SPL10* (Yu *et al.*, 2015), but the mechanisms by which these *SPL*s modulate the root system are still unclear. To investigate how miR156-targeted *SPL*s affected PR growth, we initially evaluated their expression in roots of transgenic Arabidopsis seedlings that overexpressed either miR156 (*p35S::MIR156A*) or a target mimic in which miR156 was sequestered (*p35S::MIM156* or *MIM156*) (Wu and Poethig, 2006; Franco-Zorrilla *et al.*, 2007). The transcript levels of miR156-regulated *SPL* genes (including *SPL3*, *SPL6*, *SPL9*, and *SPL10*) decreased in *p35S::MIR156A* and increased in *MIM156* roots at 10 dpg (Supplementary Fig. S3). We then examined the PR phenotypes of *p35S::MIR156A* and *MIM156* seedlings, and assessed PR growth in transgenic plants expressing the miR156-resistant versions of *SPL3*, *SPL6*, *SPL9*, and *SPL10*. We evaluated PR growth from 5 dpg because at that developmental time the meristem size has already been established (Dello Ioio *et al.*, 2008). Since root growth in these plants is reported not to be influenced by photoperiod (Yu *et al.*, 2015), all experiments were performed under long-day conditions.

At 5-dpg, the *MIM156* and *rSPL10* seedlings displayed longer PRs than the Col-0 wild-type, whereas *p35S::MIR156A* had PRs of similar length (Fig. 3A–D). This may have been because miR156 was already present at high levels in seedlings at 5dpg (Fig. 1), and *SPL* gene expression was generally repressed at this time (Fig. 2). PR lengths of *rSPL3-GUS*, *rSPL6-GUS*, and *rSPL9* seedlings at 5 dpg were similar to Col-0 (Fig. 3A–D, Supplementary Fig. S2H, I). Interestingly, *p35S::MIR156A* seedlings at 10 dpg and 15 dpg displayed shorter PRs than Col-0 (Fig. 3D). Conversely, *MIM156* and *rSPL10* seedlings consistently developed longer PRs at all developmental time points. PR length in *rSPL3-GUS*, *rSPL6-GUS*, and *rSPL9* seedlings remained similar to Col-0 at 10 and 15 dpg (Fig.

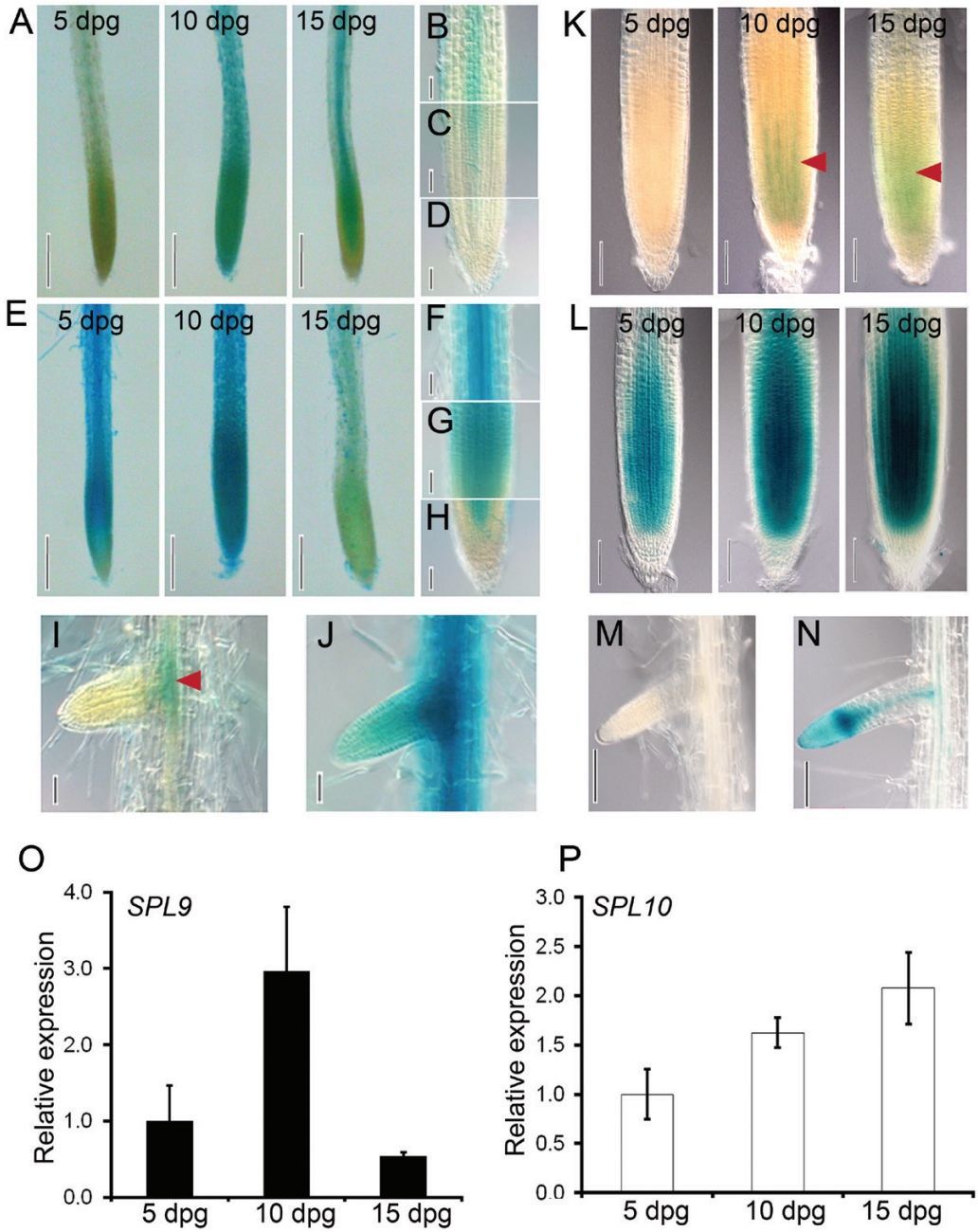

Fig. 2. Spatiotemporal expression of miR156-targeted *SPL9* and *SPL10* during the progression of root growth in Arabidopsis. Expression of the miR156-sensitive version of the *SPL9* reporter (s*SPL9-GUS*) in (A–D) primary roots (PRs) and (I) lateral root (arrowhead) at 5-, 10-, and 15-d post-germination (dpg). Expression of the miR156-resistant version of the *SPL9* reporter (*rSPL9-GUS*) in (E–H) PRs and (J) a lateral root. *SPL9* is differentially expressed during root growth. Expression of the miR156-sensitive version of the *SPL10* reporter (s*SPL10-GUS*) in (K) PRs (arrowheads) and (M) in a lateral root. Expression of the miR156-resistant version of the *SPL10* reporter (*rSPL10-GUS*) in (L) PRs and (N) a lateral root. *SPL10* is differentially expressed during root growth. (O, P) Comparative expression analysis of (O) *SPL9* and (P) *SPL10* in PRs of wild-type Col-0 seedlings as determined by qRT-PCR. Expression is relative to that of roots at 5-dpg, the value of which was set to 1. Scale bars are 250 μm (A, E) and 100 μm (B–D, F–N). The images shown are representative individuals of at least five seedlings of each genotype. Data in (O, P) are means (±SE) of three biological samples. (This figure is available in colour at *JXB* online.)

3A–D, Supplementary Fig. S2H, I). These findings suggested that at least *SPL10* was involved in modulating PR growth. To confirm this, we evaluated PR length and root meristem size in the CRISPR/Cas9-derived *spl10-2* mutant, which contains a 35-bp deletion in *SPL10* that generates a premature stop codon upstream of the SBP box (Xu *et al.*, 2016). *spl10-2* seedlings displayed shorter PR length at all the developmental times evaluated (Supplementary Fig. S4A, B). Importantly, we also found that *spl10-2* roots displayed shorter meristems compared to Col-0 (Supplementary Fig. S4C–D). These findings were surprising, given the fact that *SPL10* was only expressed at low levels in the early stages of root development (Fig. 2). Our data suggested that *SPL10* contributed to the control PR length by modulating the meristem size during the early stages of root growth. To further substantiate that the down-regulation of *SPL10* was at least partially responsible for the PR phenotype in

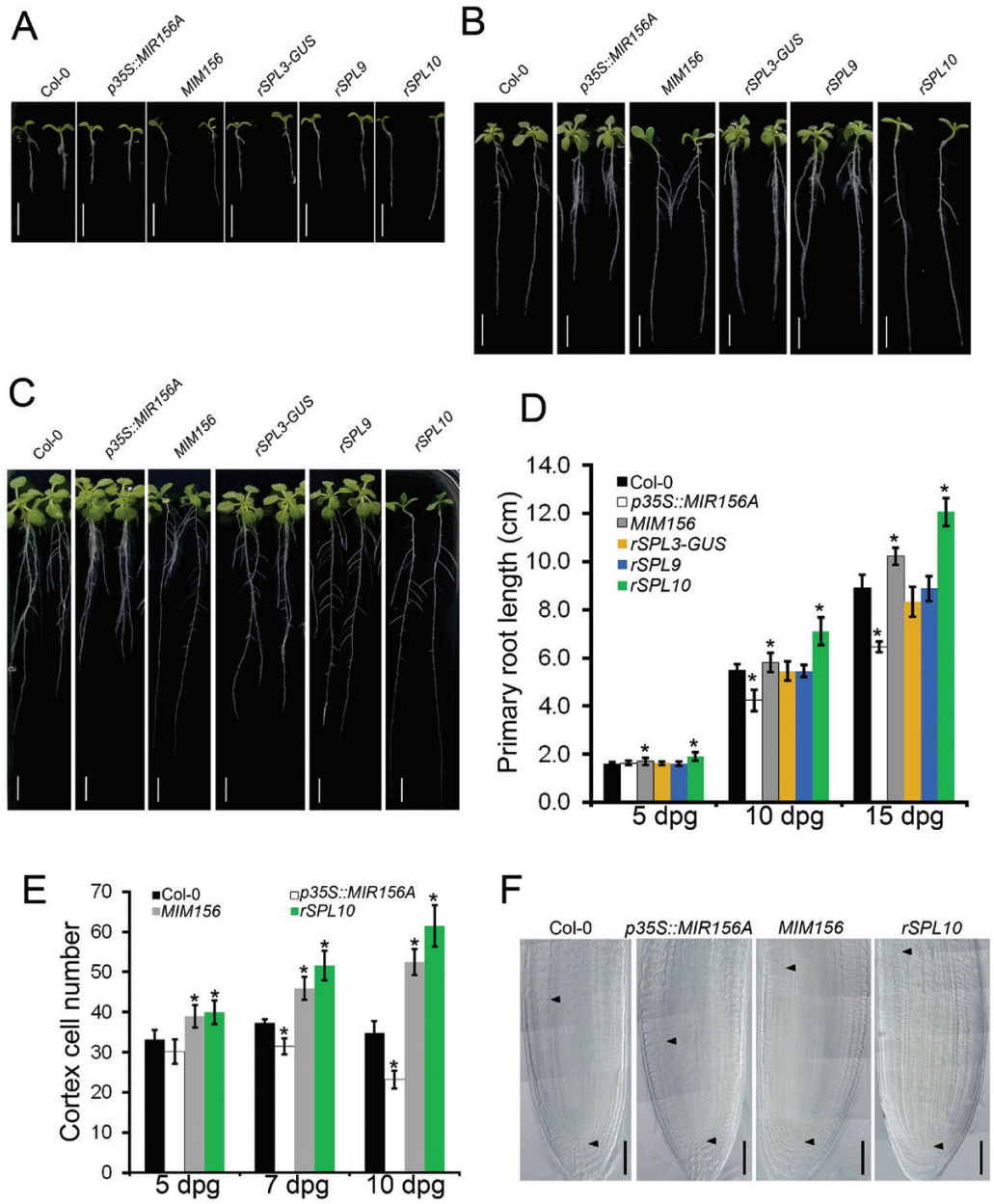

Fig. 3. Disruption of the miR156/*SPL* module in Arabidopsis affects growth of the primary root and root meristem size. (A–C) Root architecture of seedlings of wild-type Col-0, *p35S::MIR156A*, *MIM156*, *rSPL3-GUS*, *rSPL9* and *rSPL10* plants at (A) 5 d post-germination (dpg), (B) 10 dpg, and (C) 15 dpg. '*r*' indicates the miR156-resistant version of the *SPL* reporters. Scale bars are 1 cm. (D) Length of the primary roots of the seedlins shown in (A–C). Data are means (±SE) of *n*=50 seedlings. (E) Root meristem cell number of seedlings of Col-0, *p35S:: MIR156A*, *MIM156*, and *rSPL10*. Data are means (±SE) of n=20 seedlings. (F) Representative images of root meristems of Col-0, *p35S::MIR156A*, *MIM156*, and *rSPL10* seedlings at 10 dpg. Scale bars are 100 μm. Arrowheads at the bottom of the images indicate the quiescent center and those at the top indicate the cortex transition zone. Composite images were obtained using differential interference contrast microscopy as described by Dello Ioio *et al.* (2008). Significant differences in (D, E) were determined using Student's *t*-test: *$P<0.05$. (This figure is available in colour at *JXB* online.)

p35S::MIR156A seedlings (Fig. 3), we introduced the *rSPL10* construct into Arabidopsis plants harboring *p35S::MIR156A*. The de-repression of *SPL10* in the *p35S::MIR156A* seedlings was sufficient to rescue PR growth so that is was similar to Col-0 (Supplementary Fig. S4E, F). Our observations therefore confirmed the importance of the miR156:SPL ratio in the control of PR growth. In agreement with this, growth was also affected in *MIM156* seedlings in which several *SPLs* were de-repressed (Fig. 3; Supplementary Fig. S3).

High levels of miR156-resistant *SPL9* lead to shorter shoot apical meristems (Wang *et al.*, 2008). Although the expression of *SPL6* and *SPL9* was higher in the transition and meristematic zones of *rSPL6-GUS* and *rSPL9* seedlings (Fig. 2, Supplementary Fig. S2), de-repression of *SPL6* and *SPL9* did not affect PR growth or root meristem size (Fig. 3; Supplementary Figs S2J, K, S5). We next evaluated whether root meristem size was affected in *p35S::MIR156A*, *MIM156*, and *rSPL10* seedlings. As expected, the meristem size of wild-type Col-0 seedlings remained constant after 5 dpg, whereas *MIM156* and *rSPL10* had larger root meristems (Fig. 3E, F) (Dello Ioio *et al.*, 2007). In contrast, *p35S::MIR156A* displayed shorter meristems at 10 dpg and 15 dpg. This was in agreement with the root phenotypes

of the *p35S::MIR156A*, *MIM156*, and *rSPL10* seedlings (Fig. 3A–D) and suggested that the miR156/*SPL* balance had opposing effects on the root and shoot apical meristems (Wang *et al.*, 2008; Fouracre and Poethig, 2019). Interestingly, at 10 dpg and 15 dpg, root length and meristem size were slightly greater in *rSPL10* than *MIM156* seedlings (Fig. 3). This was most likely because the accumulation of *SPL10* transcripts was almost 3-fold higher in *rSPL10* than in *MIM156* roots (Fig. 4A), suggesting a quantitative effect of de-repression of *SPL10* on PR growth. In agreement with the effect of *SPL10* in modulating meristem activity, *spl10-2* roots displayed shorter meristems (Supplementary Fig. S4).

De-repression of SPL10 *increases root meristem size by affecting cell cycle activity*

The *rSPL10* seedlings consistently displayed more cortex cells in the meristematic zone (Fig. 3), suggesting that miR156-dependent de-repression of *SPL10* may have increased the division potential of the meristematic cells. To test this hypothesis, we examined the expression of the G2–M-specific *Cyclin-dependent protein kinase CYCB1;1* in Col-0 and *rSPL10* PRs at 10 dpg. To visualize *CYCB1;1* expression in *rSPL10*, we transferred the *pCYCLINB1;1::GUS* construct (Ferreira *et al.*, 1994) into *rSPL10* plants (Ubeda-Tomás *et al.*, 2008), and found an increase in the expression levels of the *pCYCB1;1::GUS* reporter in the *rSPL10* root tips (Fig. 4B). It is possible that the alterations in *CYCB1;1* expression in the *rSPL10* seedlings reflected a faster progression and/or an earlier G2/M transition of the cell cycle, thus suggesting that miR156-targeted *SPL10* may be involved in cell cycle control.

*The miR156/*SPL *module affects cell proliferation and differentiation in roots by altering auxin and cytokinin responses*

Given that the miR156/*SPL* module affected root meristem activity (Figs 3, 4), we sought to determine whether miR156-targeted *SPLs* modulate the balance between auxin and cytokinin signaling, a crucial component of meristem activity (Dello Ioio *et al.*,2008, Di Mambro *et al.*, 2017). We first investigated the auxin response by analysing the *pDR5::GFP* reporter in Col-0, *p35S::MIR156A*, and *MIM156* seedlings at 10 dpg. In the Col-0 background, *pDR5::GFP* is expressed in the quiescent center (QC) and columella cells (Fig. 5A). In the *p35S::MIR156A* background, *pDR5::GFP* was also expressed in the QC and columella layers, but apparently at slightly lower levels. In the *MIM156* background, *pDR5::GFP* was ectopically expressed, and was more laterally spread in the columella in comparison to the control. We next examined the expression levels of *PIN1*, *PIN3*, and *PIN7* by qRT-PCR. In agreement with the ectopic auxin response that was observed, *PIN1* and *PIN3* were up-regulated in *MIM156* roots, whereas no changes could be detected in the PR of *p35S::MIR156A* (Fig. 5B). This indicated that a correct miR156:SPL ratio is important but not essential for *PIN* expression. Furthermore, only particular SPLs might be involved in the regulation of these *PIN*s since no significant changes in their transcript levels were observed in the PR of *rSPL10* (Fig. 5C). We also observed that the levels of the PIN1-GFP protein were increased in the PR of *MIM156* at 10 dpg (Fig. 5D), which was in agreement with the high *PIN1* transcript levels observed (Fig. 5B). This suggested that the overall miR156-targeted de-repression of *SPL* affected auxin transport in the root meristem, at least partially by altering the expression of the transporter *PIN1*, thereby affecting the maintenance of the root meristem.

Given that *PIN1* expression was up-regulated in PRs of *MIM156* (Fig. 5B, D) and that miR156-targeted SPLs (including SPL9 and SPL10) modulate cytokinin responses through type-B ARRs (Zhang *et al.*, 2015), we investigated the effect of miR156-targeted *SPL* de-repression on cytokinin responses by evaluating *ARR1* expression in roots of Col-0, *p35S::MIR156A*, and *MIM156* at 10 dpg. While *ARR1* transcript levels were slightly higher in PRs of *p35S::MIR156A*, they were significantly reduced in *MIM156* (Supplementary Fig. S6A), suggesting a decrease in cytokinin responses. Cytokinin reduces the auxin response by activation of the transcription of *SHY2* via ARR1. SHY2 in turn negatively regulates the expression of the *PIN* genes in the roots (Dello Ioio *et al.*, 2008). We therefore measured *SHY2* expression in PRs of

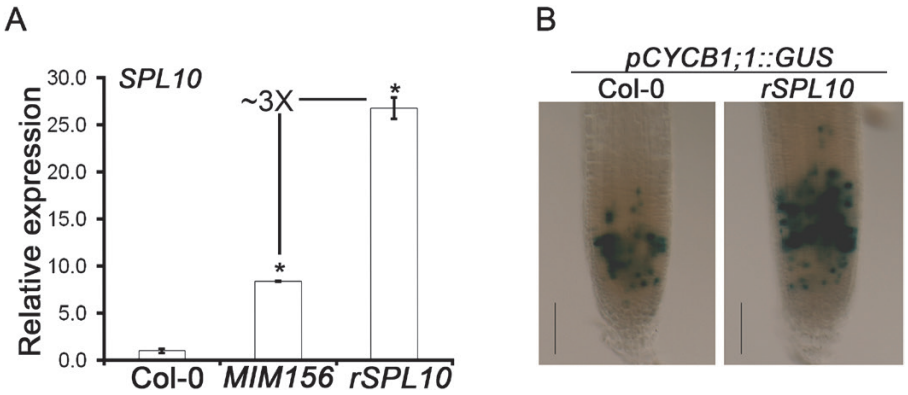

Fig. 4. De-repression of *SPL10* affects cell division rate in root meristems of Arabidopsis. (A) Comparative expression analysis of *SPL10* in roots of wild-type Col-0, *MIM156*, and *rSPL10* plants at 10 d post-germination (dpg) as determined by qRT-PCR. Expression is relative to that of Col-0, the value of which was set to 1. Data are means (±SE) of three biological samples. Significant differences were determined using the Mann–Whitney test (*P<0.05). (B) Light microscope images showing the expression of *pCYCB1;1::GUS*, a G2/M phase marker, in Col-0 and *rSPL10* roots at 10 dpg. Scale bars are 100 µm. The images are representative individuals of at least five seedlings. (This figure is available in colour at *JXB* online.)

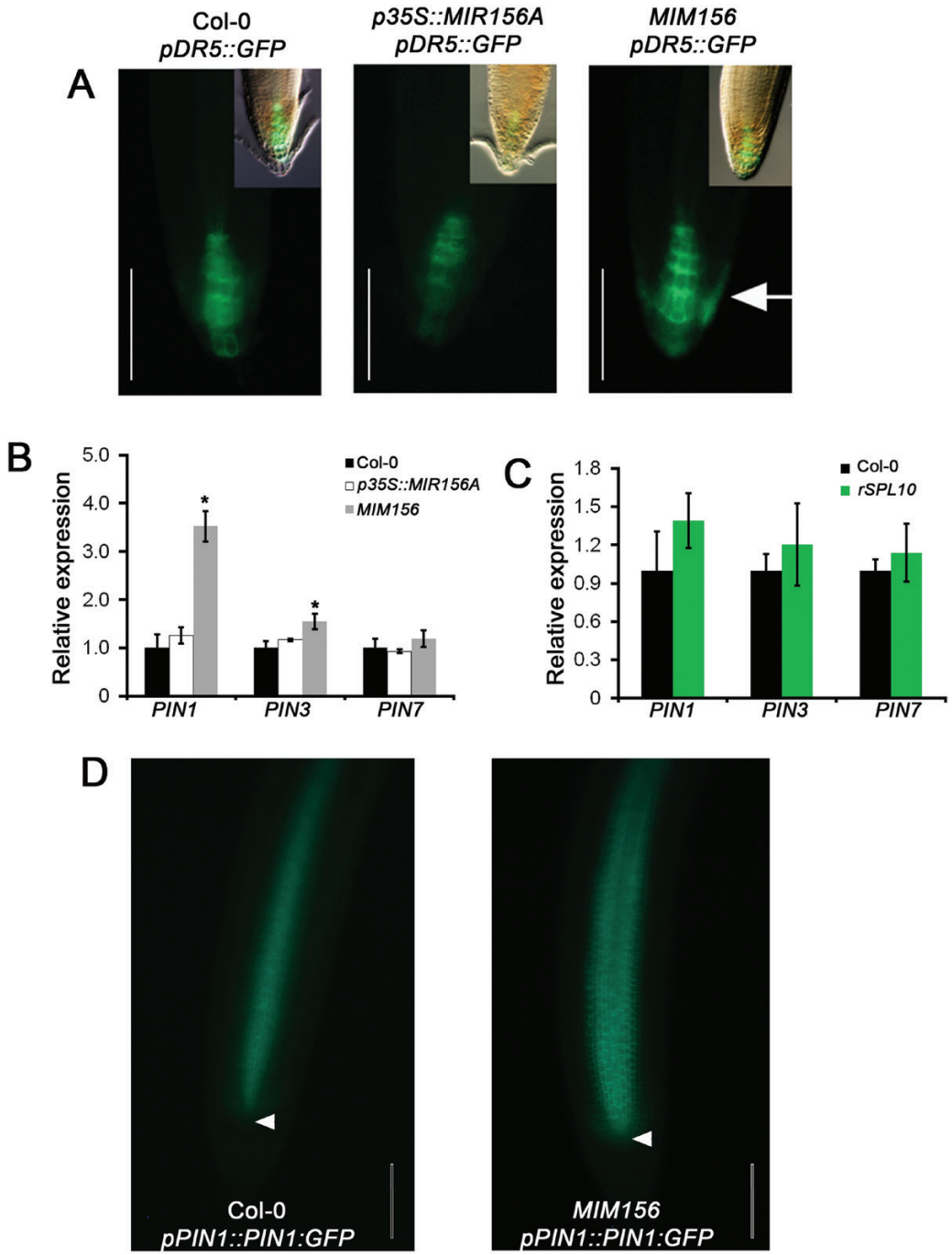

Fig. 5. The auxin response is disturbed in primary roots of *MIM156* plants of Arabidopsis. (A) Microscope images of epifluorescence in roots of *pDR5::GFP* plants at 10 d post-germination (dpg). Scale bars are 150 μm. The insets represent merged images. The arrow indicates ectopic *GFP* expression in the lateral root cap. (B, C) Comparative expression analysis of *PIN1*, *PIN3*, and *PIN7* in roots of (B) wild-type Col-0, *p35S::MIR156A*, and *MIM156*, and (C) Col-0 and *rSPL10* at 10 dpg, as determined by qRT-PCR. Expression is relative to that of Col-0, the value of which was set to 1. Data are means (±SE) of three biological samples. Significant differences compared with Col-0 were determined using the Mann–Whitney test (*P<0.05). (D) Microscope images of epifluorescence in roots of *pPIN1::PIN1:GFP* plants at 10 dpg. Scale bars are 100 μm. The arrows indicate the quiescent centers. The images are representative individuals of at least 10 seedlings. (This figure is available in colour at *JXB* online.)

Col-0, *p35S::MIR156A*, and *MIM156* at 10-dpg. Surprisingly, *SHY2* was up-regulated in *MIM156* (Supplementary Fig. S6B), suggesting that the SPL-dependent *PIN* expression (Fig. 5) was independent of the control of *SHY2* expression. We then analysed *ARR1* and *SHY2* transcript levels in *rSPL10* PR, in which *PIN* expression was similar to Col-0 (Fig. 5C) and higher cell proliferation was observed in the root meristem (Fig. 4). While *ARR1* transcript levels were strongly reduced in PRs of *rSPL10* at 10-dpg, *SHY2* expression was similar to Col-0 (Fig. 6A). Interestingly, *ARR12* was similarly expressed in *rSPL10* and Col-0. Importantly, *ARR1* was up-regulated in PRs of *spl10-2* at 10 dpg (Supplementary Fig. S4G). Together, our observations indicated that *SPL10* modulated cytokinin responses by affecting *ARR1* transcript levels. However, this modulation did not seem to result in adjustments to auxin transport, because neither *SHY2* nor *PIN* expression changed

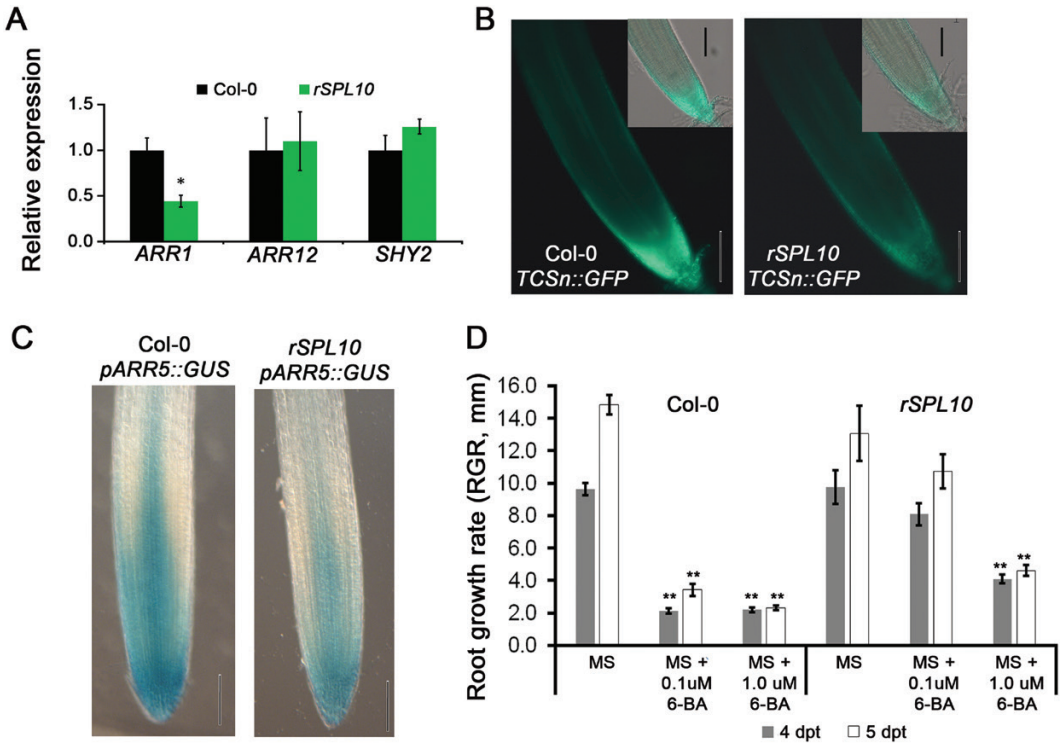

Fig. 6. De-repression of *SPL10* attenuates cytokinin responses in Arabidopsis roots. (A) Expression of *ARR1, ARR12*, and *SHY2* in roots of wild-type Col-0 and *rSPL10* seedlings at 10 d post-germination (dpg), as determined by qRT-PCR.Expression is relative to that of Col-0, the value of which was set to 1. Data are means (±SE) of three biological samples. Significant differences compared with Col-0 were determined using the Mann–Whitney test (*P<0.05) (B) Microscope images of epifluorescence of *TCSn::GFP* expression in roots at 10 dpg. Scale bars are 100 μm. The insets represent merged images. (C) Expression of *pARR5::GUS* in Col-0 and *rSPL10* seedlings at 10 dpg. Scale bars are 100 μm. (D) Root growth rate (RGR) of Col-0 and *rSPL10* seedlings growing in MS medium with or without 6-benzyladenine (6-BA). RGR was evaluated at 4 d and 5 d post-treatment (dpt). Data are means (±SE) of n=45 seedlings. Significant differences compared with untreated MS medium were determined using Student's t-test: **P<0.01. The experiment was repeated three times with similar results. (This figure is available in colour at *JXB* online.)

in the PRs of *rSPL10* (Figs 5C, 6A). To further elucidate the interplay between *SPL10* and *ARR1*-mediated cytokinin responses, we introduced the *arr1-4* allele (Dello Ioio *et al.*, 2007) into *rSPL10* plants to generate *rSPL10*;*arr1-4* plants. *rSPL10*;*arr1-4* seedlings displayed longer PRs and larger root meristems that were similar to phenotypes of *rSPL10* and *arr1-4* seedlings (Supplementary Fig. S7). These findings indicated that *SPL10* in *ARR1* acted in similar genetic pathways in controlling PR growth.

To further substantiate the role of SPL10 in modulating cytokinin responses in PRs, we compared the responses to cytokinin in Col-0 and *rSPL10* by using the *Two Component signaling Sensor new* (*TCSn*)*::GFP* reporter, which reflects the transcriptional activity of type-B *ARR*s (Müller and Sheen, 2008; Zürcher *et al.*, 2013). We also analysed the widely used *pARR5::GUS* cytokinin reporter (D'Agostino *et al.*, 2000). In the PRs of Col-0, *GFP* expression was observed in the columella cells of the root meristem and in the vasculature, whereas lower GFP levels were observed in similar cell types of *rSPL10* PR (Fig. 6B) (Zürcher *et al.*, 2013). Likewise, lower *pARR5::GUS* activity was detected in *rSPL10* compared to Col-0 (Fig. 6C).

Exogenous cytokinin application reduces root meristem size and overall PR growth (Dello Ioio *et al.*, 2007). We hypothesized that the low response to cytokinin observed in *rSPL10* (Fig. 6A–C) may lead to a decrease in the effects of exogenous cytokinin. We therefore treated Col-0 and *rSPL10* seedlings with two concentrations of 6-benzyladenine (6-BA), a synthetic cytokinin (Dello Ioio *et al.*, 2007), and examined the growth rate of the PR (RGR) at 4 d and 5 d post-treatment (dpt; Supplementary Fig. S8)). Interestingly, RGR was similar between Col-0 and *rSPL10* growing in control MS medium at 4 dpt and 5-dpt (Fig. 6D). At the low 6-BA concentration (0.1 μM), RGR was lower in Col-0 than in *rSPL10* at both 4-dpt and 5-dpt, suggesting that *rSPL10* seedlings were less sensitive to this cytokinin treatment. At the higher 6-BA concentration (1.0 μM), the differences were less pronounced, but the PRs of *rSPL10* were again less affected than Col-0. Overall, these results supported the idea that de-repression of *SPL10* leads to lower cytokinin responses in roots, thus inducing a higher rate of cell proliferation in the root meristem.

The miR156/SPL module controls root-derived de novo *shoot organogenesis via cytokinin responses*

The miR156/SPL module influenced the growth of PRs by altering cytokinin and auxin responses (Figs 5, 6). Emergence of LRs is also affected by the miR156/SPL module (Yu *et al.*, 2015), probably also through the modulation of cytokinin and auxin responses. Because LR formation and *de novo* shoot organogenesis (DNSO) from PRs share their initial developmental stages and because a correct auxin:cytokinin balance is

crucial for DNSO (Atta *et al.*, 2009; Sugimoto *et al.*, 2010), we investigated the roles of the miR156/SPL module on DNSO from root explants.

We performed *in vitro* regeneration assays in which root explants were submitted to the traditional two-step regeneration procedure (Valvekens *et al.*, 1988). In the first step, callus is induced from explants cultured on auxin-rich callus-inducing medium (CIM). Subsequently, the explants were transferred to shoot-inducing medium (SIM) containing a high cytokinin:auxin ratio for inducing the differentiation of the callus into shoots (Valvekens *et al.*, 1988; Duclercq *et al.*, 2011). Given that miR156, *SPL9*, and *SPL10* transcription is activated by auxin in roots (Yu *et al.*, 2015), we evaluated their expression patterns in intact PRs of Col-0 at 7 dpg and compared them with root explants that had undergone different steps in the regeneration process: 4 d in CIM (which contained high levels of dichlorophenoxyacetic acid or 2,4-D; Atta *et al.*, 2009) and 6 d in SIM. While transcripts of *SPL9* and *SPL10* accumulated at high levels in root explants under both CIM and SIM incubation compared to PRs at 7 dpg, miR156 transcripts were only higher in the auxin-rich CIM medium (Supplementary Fig. S9). The high expression of miR156 and *SPLs* in the CIM medium indicated that both miR156 and its targets were positively regulated by 2,4-D during the callus-induction stage, similar to their regulation by IAA in roots (Yu *et al.*, 2015).

We next evaluated the shoot regenerative capacity of root explants obtained from Col-0, *p35S::MIR156A*, *rSPL9*, and *rSPL10* seedlings at 7 dpg and 10 dpg (Fig. 7A). De-repression of *SPL9* markedly reduced shoot regeneration in *rSPL9* roots (Fig. 7B, C), similar to previous reports for aerial tissues (Zhang *et al.*, 2015). Strikingly, the de-repression of *SPL10* completely abolished DNSO in both 7 dpg and 10 dpg *rSPL10* explants. These observations were consistent with the roles of *SPL9* and *SPL10* in controlling LR emergence (Yu *et al.*, 2015) and indicated that *SPL10* has a major role in regulating common pathways that control LR emergence and DNSO. Interestingly, we observed that *p35S::MIR156A* roots at 7 dpg and 10 dpg had a lower number of regenerated shoots compared with the wild-type Col-0 (Fig. 7B, C), in contrast to *p35S::MIR156A* that has been shown to have higher regenerative capacity in aerial tissues (i.e. leaves and hypocotyls; Zhang *et al.*, 2015). Higher levels of miR156 reduce the number of LR primordia (stages I–IV) but increase the number of emerged LRs compared with Col-0 (Supplementary Fig. S10; Yu *et al.*, 2015). It may be speculated that fewer 'founder cells' necessary for DNSO (Motte *et al.*, 2014) are specified in miR156-overexpressing roots, perhaps due to the lower auxin response (Fig. 5A). On the other hand, the lower regenerative capacity of *rSPL9* roots (Fig. 7) might be a result of reduced emergence of regenerated shoots (Yu *et al.*, 2015; Zhang *et al.*, 2015). These suggestions are worthy of further investigation.

Although DNSO was severely impaired in *rSP10* roots (Fig. 7), meristemoid-like structures were generated in them (Fig. 8D–F), and these were not seen in Col-0 (Fig. 8A–C). SEM revealed that these meristemoid-like structures contain stomata, which indicated premature epidermal differentiation of these structures compared with leaves derived from Col-0 shoots (Fig. 8C, F). To gain more insight on how these meristemoid-like structures are generated in *rSPL10* root explants, we examined longitudinal sections of explants cultured in CIM and SIM. After 4 d of incubation in CIM, Col-0 and *rSPL10* explants displayed similar periclinal cell divisions originating from the pericycle tissue (Fig. 8G, J). However, after 10 d of

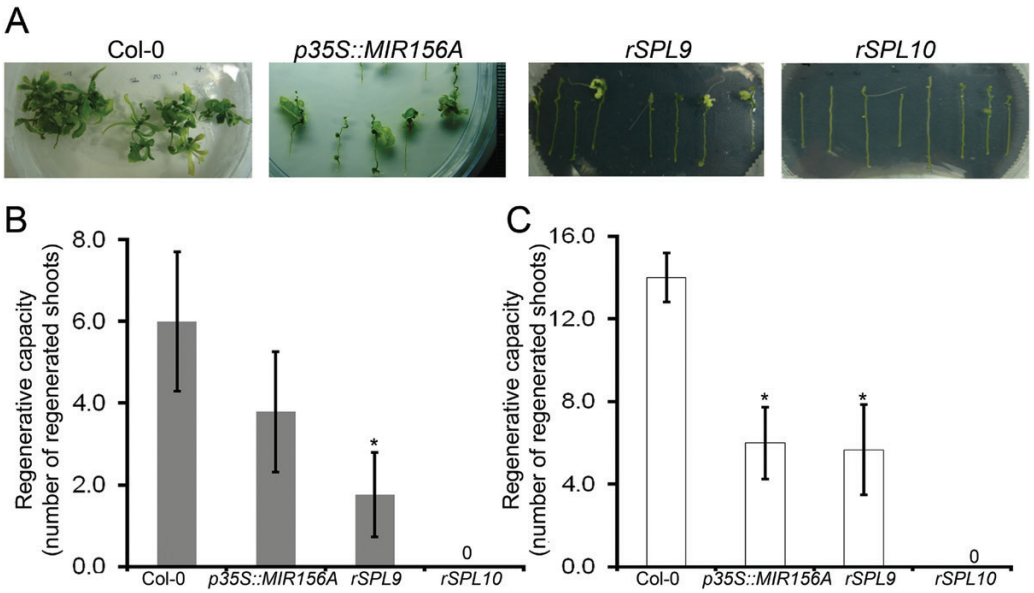

Fig. 7. miR156-dependent regulation of *SPL*s is required for root-derived *de novo* shoot organogenesis in Arabidopsis. (A) Shoot regeneration assays using root explants from wild-type Col-0, *p35S::MIR156A*, *rSPL9*, and *rSPL10* seedlings at 7 d post-germination (dpg). Root explants were cultured for 4 d on callus-induction medium and then transferred to shoot-induction medium (SIM) for 20 d. (B, C) Quantitative analyses of regenerative capacity of the seedlings at (B) 7 dpg and (C) 10 dpg. The regenerative capacity is represented by the mean number of regenerated shoots after 20 d in SIM. Data are means (±SE) of three biological replicates. Significant differences compared with Col-0 were determined using Student's *t*-test (*P<0.05). The experiment was repeated three times with similar results. (This figure is available in colour at *JXB* online.)

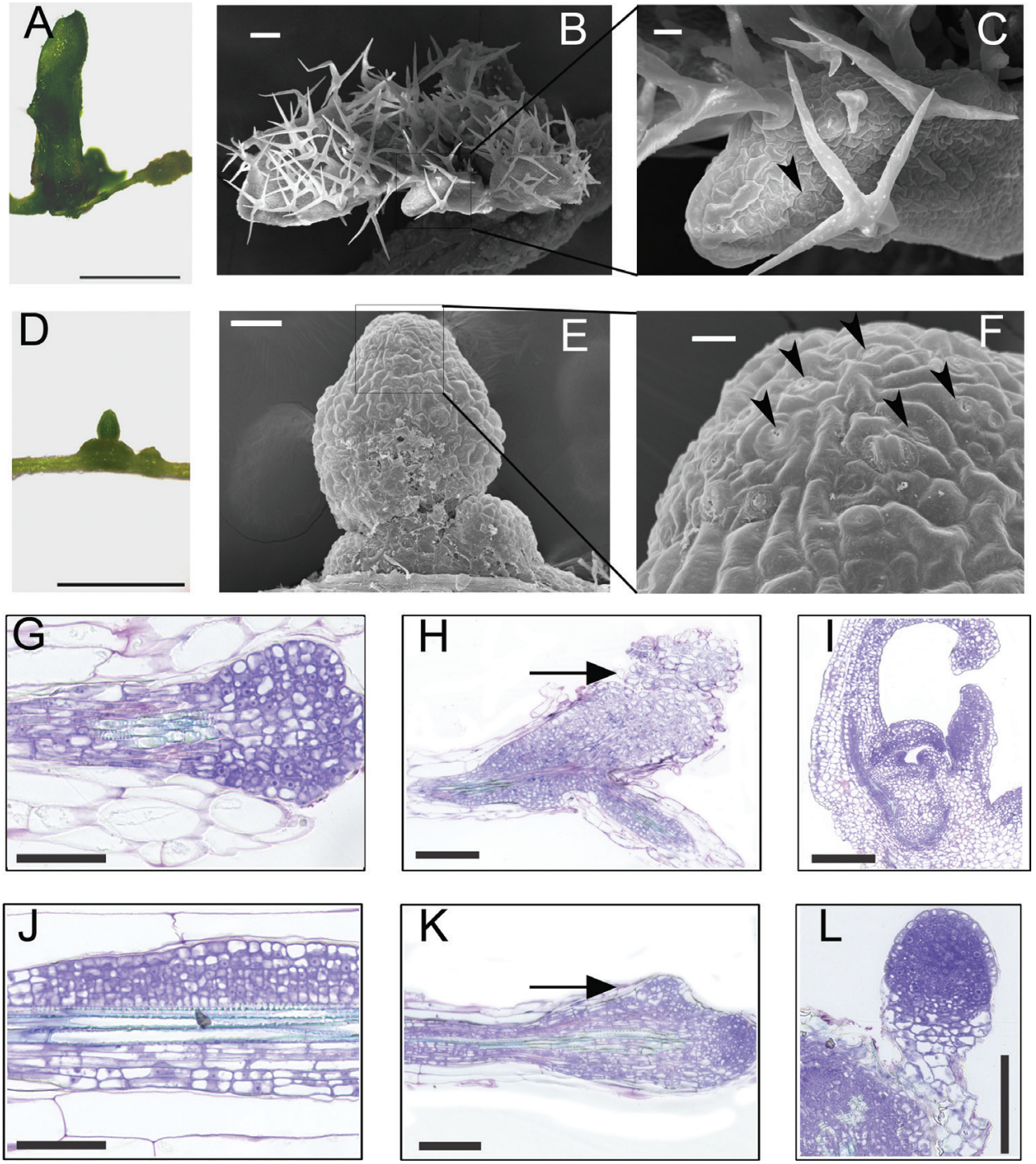

Fig. 8. De-repression of miR156-targeted *SPL10* abolishes shoot regeneration in Arabidopsis. (A, D) Representative images of regenerated shoots from root explants of (A) wild-type Col-0 and (D) *rSPL10*. Scale bars are 1 mm. SEM images of regenerated shoots from (B, C) Col-0 and (E, F) *rSPL10*; (C, F) are magnifications of the regions marked in (B, E). Arrowheads indicate stomata. Scale bars are 100 μm (B, E) and 20 μm (C, F). Longitudinal sections of (G–I) Col-0 root explants cultured for (G) 4 d in callus-induction medium (CIM), and then cultured in shoot-induction medium (SIM) for (H) 10 d and (I) 20 d. Longitudinal sections of *rSPL10* root explants cultured for (J) 4 d in CIM, and then cultured in SIM for 10 d and (L) 20 d. Scale bars are 100 μm (G–K) and 200 μm (L). (This figure is available in colour at *JXB* online.)

cultivation in SIM, Col-0 showed an intense formation of cellular mass (callus) protruding from the root explants (Fig. 8H) whereas *rSPL10* did not show any apparent formation of cellular mass (Fig. 8K). This might indicate a decrease in cell division in *rSPL10* explants when cultured in the cytokinin-rich SIM. After 20 d of incubation in SIM, a shoot apical meristem and leaf primordia were visible in shoots derived from Col-0 (Fig. 8I), but not in those from *rSPL10* root explants (Fig. 8L).

Loss-of-function mutants for type-B *ARR*s, including *ARR1* and *ARR2*, display decreased cell division and shooting in tissue culture, whilst their increased expression enhances the response to cytokinin in tissue culture (Hwang and Sheen,

2001; Sakai *et al.*, 2001; Duclercq *et al.*, 2011). Thus, it is possible that the reduced cell division and premature cell/tissue differentiation observed in *rSP10*-derived *in vitro* structures may have been a result of the down-regulation of *ARR1* in the roots (Fig. 6A), resulting in the attenuation of the cytokinin response. To test this hypothesis, we evaluated *pARR5::GUS* expression in root explants of Col-0, *p35S::MIR156A*, and *rSPL10* after incubation in CIM and SIM media (Fig. 9). After 2 d in the SIM, *GUS* staining was stronger in the *p35S::MIR156A;pARR5::GUS* explants compared with Col-0;*pARR5::GUS* (Fig. 9A). Conversely, lower *GUS* staining was observed in *rSPL10;pARR5::GUS* explants. These observations indicated that even in SIM (which contained a high cytokinin:auxin ratio; Valvekens *et al.*, 1988), the cytokinin response was impaired in *rSPL10* root explants. To further substantiate this finding, we tested the regenerative capacity of the roots in different cytokinin (2-iP) concentrations. As expected, increasing cytokinin concentration in the SIM correlated with higher regenerative capacity from Col-0 root explants, but it did not improve the low regenerative capacity of *p35S::MIR156A*. Most importantly, elevation of cytokinin in the SIM was not able to restore the regenerative capacity of *rSPL10* root explants (Fig. 9B–E). Together, these results indicated that the unbalance between miR156 and *SPL10* levels was sufficient to modify root-derived shoot regenerative capacity via attenuating cytokinin responses.

Discussion

MiR156 and its targets are the master regulators of phase change, and this has been confirmed by numerous reports that have mostly focused on the aerial organs (Schwarz *et al.*, 2008; Wang *et al.*, 2008; Usami *et al.*, 2009; Wu *et al.*, 2009; Yu *et al.*, 2010; Silva *et al.*, 2019). Our results suggested that miR156 and *SPL*s also play a role in the growth of PRs during the progression of seedling development. *MIR156A* and *MIR156C* (Yang *et al.*, 2013; Xu *et al.*, 2018) were expressed in roots and their transcription levels decreased as the seedling aged (Fig. 1). *SPL*s such as *SPL9* and *SPL10* have regulatory sequences that can drive their transcription across a broad region (Xu *et al.*, 2016), most noticeably in the root meristematic and transition zones (Fig. 2). Our results demonstrate that post-transcriptional repression by miR156 is necessary to achieve

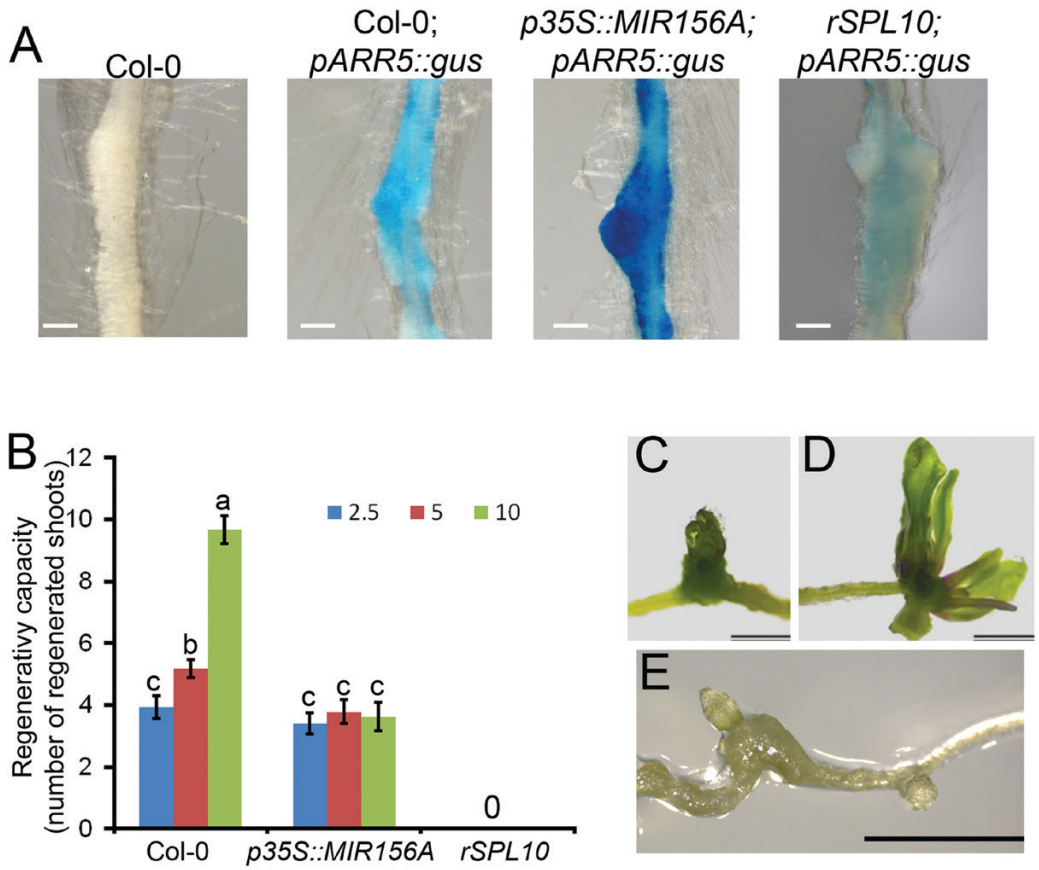

Fig. 9. De-repression of miR156-targeted *SPL*s affects cytokinin responses during *in vitro* shoot organogenesis in Arabidopsis. (A) Representative images of root explants from wild-type Col-0, Col-0;*pARR5::GUS*, *p35S::MIR156A*;*pARR5::GUS*, and *rSPL10*;*pARR5::GUS* seedlings incubated in shoot-induction medium (SIM) for 2 d. Scale bars are 500 μm. (B) Quantitative analyses of regenerative capacity of root explants of Col-0, *p35S::MIR156A*, and *rSPL10* incubated in SIM supplemented with 2.5 μM, 5 μM, or 10 μM of isopentenyladenine (2-iP). The regenerative capacity is represented by the mean number of regenerated shoots after 20 d in SIM. Different letters indicate significant differences according to ANOVA followed by Tukey's HSD test ($P<0.05$). Data are means (±SE) from three replicates of two independent experiments. (C–E) Representative images of regenerated organs (shoots and meristemoid-like structures) from root explants of (C) Col-0, (D) *p35S::MIR156A*, and (E) *rSPL10* incubated in SIM supplemented with 5 uM 2-iP. Scale bars are 2 mm. (This figure is available in colour at *JXB* online.)

the correct spatiotemporal expression patterns of the *SPLs* during the progression of root growth (Fig. 2, Supplementary Figs S1, S2). Importantly, miR156 activity was detected in the elongation and meristematic zones, suggesting its role in regulating the expression of some *SPLs* in these regions (Fig. 1). miR156-targeted *SPLs* might also have a role in delineating the region between the elongating and mature root cells since they have higher and lower expression, respectively, in these zones, whilst miR156 shows the opposite expression pattern (Breakfield *et al.*, 2012).

The correct balance between the rates of cell division and differentiation determines the size of the root meristem and the rate of root growth (Dello Ioio *et al.*, 2007). Roots with miR156-overpression and miR156-target mimicry displayed lower and higher meristem cell numbers, respectively (Fig. 3), suggesting that a correct threshold-dependent repression of *SPL* expression by miR156 (He *et al.*, 2018) contributes to regulate the balance between cell proliferation and differentiation. In Arabidopsis leaves, *SPLs* that promote heteroblasty, namely *SPL3*, *-4*, *-5*, and *-15*, increase cell number and reduce cell size (Usami *et al.*, 2009); however, how they regulate this is not yet clear. In developing roots, *SPL10*-dependent modulation of meristematic cell division may occur through two overlapping mechanisms: (1) directly by increasing the overall division rate (visualized by the higher *pCYCB1;1::GUS* expression in *rSPL10* roots; Fig. 4); and (2) indirectly by attenuating the cytokinin responses in the roots (visualized by the intensity of cytokinin signaling, as assayed by *TCSn::GFP* and *pARR5:GUS* reporters and by the down-regulation of *ARR1*; Fig. 6). Our observations were consistent with the role of cytokinins in controlling the rate of meristematic cell differentiation (Dello Ioio *et al.*, 2007, 2008; Di Mambro *et al.*, 2017). In addition, the overall de-repression of miR156-targeted *SPLs* may also have affected meristem size and PR growth through auxin signaling, since *MIM156* roots presented high levels of *PIN1* expression and showed an ectopic auxin response (Fig. 5).

Zhang *et al.* (2015) reported that miR156-targeted SPL9 as well as SPL10 directly bind to the type-B ARR2 protein, lessening the cytokinin responses (Heyl and Schmülling, 2003). This is consistent with our observations that *TCSn::GFP* and *pARR5::GUS* reporter levels were reduced in PRs of *rSPL10* (Fig. 6), which is also in agreement with the fact that type-A *ARR*s, including *ARR5*, were induced by 6-BA treatment in *p35S::MIR156A* but reduced in *MIM156* plants (Zhang *et al.*, 2015). The transcriptional activator type-B *ARR1* is crucial for controlling most of the genes under cytokinin regulation (Argyros *et al.*, 2008). *ARR1* transcript levels were reduced in *MIM156* and *rSPL10* roots (Fig. 6, Supplementary Fig. S6). This suggests that, in addition to regulating ARR transcriptional activity (Zhang *et al.*, 2015), miR156-targeted SPLs, including SPL10, may modulate cytokinin-responsive genes in roots via *ARR1* transcriptional regulation. However, whether this is achieved by a direct or indirect regulation of *ARR1* requires further investigation.

Cytokinin responses mediated by the miR156/*SPL* module also controlled *in vitro* regeneration (Fig. 7). Aerial tissues of young Arabidopsis plants exhibited high cytokinin responses and DNSO, due to the high levels of miR156. Conversely, high levels of SPLs directly inhibited the transcriptional activity of type-B ARRs, thus impairing shoot regenerative capacity. As a result, aerial explants from plants expressing miR156-resistant versions of *SPLs* (*rSPLs*) display low regenerative capacity (Zhang *et al.*, 2015). Similarly, root-derived explants from *rSPL9* and *rSPL10* displayed low and no regenerative capacity, respectively (Fig. 7). The role of *SPL10* in DNSO has not previously been investigated, and we show here that the de-repression of *SPL10* in *rSPL10* plants completely abolished the shoot regenerative capacity of roots (Figs. 7–9). This loss of regenerative capacity in *rSPL10* was more severe than that observed for *rSPL9* plants, which were still able to generate shoots from aerial explants (Zhang *et al.*, 2015) and from roots (Fig. 7). Although the direct targets of *SPL10* in roots still need to be identified, the disruption of miR156-mediated regulation of *SPL10* in Arabidopsis induces genes associated with seed maturation before the embryo has been formed (Nodine and Bartel, 2010). Similarly, the premature differentiation of meristemoid-like structures in PRs of *rSPL10* (Fig. 8) might be a result of a precocious induction of genes associated with DNSO. This precocious induction is likely to be coupled to changes in cytokinin levels/responses, since exogenous and endogenous cytokinins influence the initiation of newly formed organs, as well as the pace of organ development (Pernisova *et al.*, 2018). The lower expression of *pARR5::GUS* and the high insensitivity of *rSPL10* root explants to cytokinin treatment (Fig. 9) strongly indicated that *SPL10*-dependent DNSO from roots occurs mostly through modulation of the cytokinin signaling. It is possible that the fundamental role of *SPL10* in root-derived DNSO (Fig. 7–9) overlaps with its role in modulating LR development (Yu *et al.*, 2015).

In conclusion, our data suggest that the balance between meristem activity and lateral organ development in roots may be achieved by the maintenance of a correct miR156:SPL ratio during early stages of development.

Supplementary data

Supplementary data are available at *JXB* online.

Fig. S1. MiR156-targeted *SPL3* is expressed in primary and lateral roots.

Fig. S2. MiR156-targeted *SPL6* is expressed in PRs but it does not affect meristem size and root length.

Fig. S3. *SPLs* are down- and up-regulated in *p35S::MIR156A* and *MIM156* roots, respectively.

Fig. S4. PR length and meristem size are reduced in the *spl10-2* mutant.

Fig. S5. MiR156-targeted *SPL9* de-repression does not affect root meristem size.

Fig. S6. De-repression of miR156-targeted *SPL* decreases the expression of type-B *ARR1* in roots.

Fig. S7. *SPL10* and *ARR1* act in similar genetic pathways during root growth.

Fig. S8. Representative images of *rSPL10* and Col-0 seedlings in response to treatment with 6-benzyladenine.

Fig. S9. MiR156-targeted *SPL9* and *SPL10* as well as the mature miR156 are up-regulated in auxin-rich medium.

Fig. S10. *MIR156* overexpression increases the number of lateral roots as early as 5 d post-germination.

Table S1. Oligonucleotide sequences used in this work.

Acknowledgements

We thank the members of Dr Nogueira's laboratory for helpful discussions. We are indebted to Scott Poethig (University of Pennsylvania), Michael Nodine (Gregor Mendel Institute of Molecular Plant Biology), Yuke He (Shanghai Institute of Plant Physiology and Ecology), Paulo Ferreira (Federal University of Rio de Janeiro), and Bruno Müller (University of Zurich) for providing plant material. CHB-R was the recipient of a National Council for Scientific and Technological Development (CNPq) fellowship. This work was supported by The São Paulo Research Foundation FAPESP (grant nos. 15/17892–7 and 18/17441–3). The authors declare no conflict of interest.

Author contributions

FTSN, CHB-R, and GHBR conceived the research; CHB-R, GHBR, LP, DAPB, DSB, MMN, ACFC, and EGOM devised the methodology; CHB-R, GHBR, LP, DAPB, DSB, and MMN conducted the experiments; FTSN, SS, and WCO analysed the data; FTSN and CHB-R wrote the original draft of the paper; FTSN, CHB-R, SS, and WCO revised and edited the paper; FTSN supervised the research, administered the project, and acquired the funding; all authors read and approved the final manuscript.

References

Argyros RD, Mathews DE, Chiang YH, Palmer CM, Thibault DM, Etheridge N, Argyros DA, Mason MG, Kieber JJ, Schaller GE. 2008. Type B response regulators of *Arabidopsis* play key roles in cytokinin signaling and plant development. The Plant Cell **20**, 2102–2116.

Atta R, Laurens L, Boucheron-Dubuisson E, Guivarc'h A, Carnero E, Giraudat-Pautot V, Rech P, Chriqui D. 2009. Pluripotency of Arabidopsis xylem pericycle underlies shoot regeneration from root and hypocotyl explants grown *in vitro*. The Plant Journal **57**, 626–644.

Beemster GT, Baskin TI. 1998. Analysis of cell division and elongation underlying the developmental acceleration of root growth in *Arabidopsis thaliana*. Plant Physiology **116**, 1515–1526.

Bharathan G, Goliber TE, Moore C, Kessler S, Pham T, Sinha NR. 2002. Homologies in leaf form inferred from *KNOXI* gene expression during development. Science **296**, 1858–1860.

Blilou I, Xu J, Wildwater M, Willemsen V, Paponov I, Friml J, Heidstra R, Aida M, Palme K, Scheres B. 2005. The PIN auxin efflux facilitator network controls growth and patterning in *Arabidopsis* roots. Nature **433**, 39–44.

Breakfield NW, Corcoran DL, Petricka JJ, Shen J, Sae-Seaw J, Rubio-Somoza I, Weigel D, Ohler U, Benfey PN. 2012. High-resolution experimental and computational profiling of tissue-specific known and novel miRNAs in *Arabidopsis*. Genome Research **22**, 163–176.

Burstrom H. 1957. Auxin and the mechanism of root growth. Symposia of the Society for Experimental Biology **11**, 44–62.

Carlsbecker A, Lee JY, Roberts CJ, *et al*. 2010. Cell signalling by microRNA165/6 directs gene dose-dependent root cell fate. Nature **465**, 316–321.

Che P, Lall S, Howell SH. 2007. Developmental steps in acquiring competence for shoot development in *Arabidopsis* tissue culture. Planta **226**, 1183–1194.

Clough SJ, Bent AF. 1998. Floral dip: a simplified method for *Agrobacterium*-mediated transformation of *Arabidopsis thaliana*. The Plant Journal **16**, 735–743.

Couzigou JM, Combier JP. 2016. Plant microRNAs: key regulators of root architecture and biotic interactions. New Phytologist **212**, 22–35.

Czechowski T, Stitt M, Altmann T, Udvardi MK, Scheible WR. 2005. Genome-wide identification and testing of superior reference genes for transcript normalization in Arabidopsis. Plant Physiology **139**, 5–17.

D'Agostino IB, Deruère J, Kieber JJ. 2000. Characterization of the response of the *Arabidopsis* response regulator gene family to cytokinin. Plant Physiology **124**, 1706–1717.

Dastidar MG, Jouannet V, Maizel A. 2012. Root branching: mechanisms, robustness, and plasticity. WIREs Developmental Biology **1**, 329–343.

De Smet I, Lau S, Voss U, *et al*. 2010. Bimodular auxin response controls organogenesis in *Arabidopsis*. Proceedings of the National Academy of Sciences, USA **107**, 2705–2710.

De Smet I, Tetsumura T, De Rybel B, *et al*. 2007. Auxin-dependent regulation of lateral root positioning in the basal meristem of *Arabidopsis*. Development **134**, 681–690.

Dello Ioio R, Linhares FS, Scacchi E, Casamitjana-Martinez E, Heidstra R, Costantino P, Sabatini S. 2007. Cytokinins determine *Arabidopsis* root-meristem size by controlling cell differentiation. Current Biology **17**, 678–682.

Dello Ioio R, Nakamura K, Moubayidin L, Perilli S, Taniguchi M, Morita MT, Aoyama T, Costantino P, Sabatini S. 2008. A genetic framework for the control of cell division and differentiation in the root meristem. Science **322**, 1380–1384.

Di Mambro R, De Ruvo M, Pacifici E, *et al*. 2017. Auxin minimum triggers the developmental switch from cell division to cell differentiation in the Arabidopsis root. Proceedings of the National Academy of Sciences, USA **114**, E7641–E7649.

Duclercq J, Sangwan-Norreel B, Catterou M, Sangwan RS. 2011. *De novo* shoot organogenesis: from art to science. Trends in Plant Science **16**, 597–606.

Ferreira PC, Hemerly AS, Engler JD, van Montagu M, Engler G, Inzé D. 1994. Developmental expression of the Arabidopsis cyclin gene *cyc1At*. The Plant Cell **6**, 1763–1774.

Fouracre JP, Poethig RS. 2019. Role for the shoot apical meristem in the specification of juvenile leaf identity in *Arabidopsis*. Proceedings of the National Academy of Sciences, USA **116**, 10168–10177.

Franco-Zorrilla JM, Valli A, Todesco M, Mateos I, Puga MI, Rubio-Somoza I, Leyva A, Weigel D, García JA, Paz-Ares J. 2007. Target mimicry provides a new mechanism for regulation of microRNA activity. Nature Genetics **39**, 1033–1037.

Fukaki H, Tameda S, Masuda H, Tasaka M. 2002. Lateral root formation is blocked by a gain-of-function mutation in the *SOLITARY-ROOT/IAA14* gene of *Arabidopsis*. The Plant Journal **29**, 153–168.

Gamborg OL, Miller RA, Ojima K. 1968. Nutrient requirements of suspension cultures of soybean root cells. Experimental Cell Research **50**, 151–158.

Gifford ML, Dean A, Gutierrez RA, Coruzzi GM, Birnbaum KD. 2008. Cell-specific nitrogen responses mediate developmental plasticity. Proceedings of the National Academy of Sciences, USA **105**, 803–808.

Guo HS, Xie Q, Fei JF, Chua NH. 2005. MicroRNA directs mRNA cleavage of the transcription factor NAC1 to downregulate auxin signals for arabidopsis lateral root development. The Plant Cell **17**, 1376–1386.

Guo AY, Zhu QH, Gu X, Ge S, Yang J, Luo J. 2008. Genome-wide identification and evolutionary analysis of the plant specific SBP-box transcription factor family. Gene **418**, 1–8.

He J, Xu M, Willmann MR, McCormick K, Hu T, Yang L, Starker CG, Voytas DF, Meyers BC, Poethig RS. 2018. Threshold-dependent repression of *SPL* gene expression by miR156/miR157 controls vegetative phase change in *Arabidopsis thaliana*. PLoS Genetics **14**, e1007337.

Heyl A, Schmülling T. 2003. Cytokinin signal perception and transduction. Current Opinion in Plant Biology **6**, 480–488.

Hodge A. 2006. Plastic plants and patchy soils. Journal of Experimental Botany **57**, 401–411.

Hwang I, Sheen J. 2001. Two-component circuitry in *Arabidopsis* cytokinin signal transduction. Nature **413**, 383–389.

Jones-Rhoades MW, Bartel DP, Bartel B. 2006. MicroRNAs and their regulatory roles in plants. Annual Review of Plant Biology **57**, 19–53.

Jurado S, Abraham Z, Manzano C, López-Torrejón G, Pacios LF, Del Pozo JC. 2010. The *Arabidopsis* cell cycle F-box protein SKP2A binds to auxin. The Plant Cell **22**, 3891–3904.

Karnovsky MJ. 1965. A formaldehyde-glutaraldehyde fixative of high osmolality for use in electron microscopy. Journal of Cellular Biology **27**, 137–138.

Lagos-Quintana M, Rauhut R, Lendeckel W, Tuschl T. 2001. Identification of novel genes coding for small expressed RNAs. Science **294**, 853–858.

Li S, Yang X, Wu F, He Y. 2012. HYL1 controls the miR156-mediated juvenile phase of vegetative growth. Journal of Experimental Botany **63**, 2787–2798.

Livak KJ, Schmittgen TD. 2001. Analysis of relative gene expression data using real-time quantitative PCR and the $2^{-\Delta\Delta C^T}$ method. Methods **25**, 402–408.

Mallory AC, Dugas DV, Bartel DP, Bartel B. 2004. MicroRNA regulation of NAC-domain targets is required for proper formation and separation of adjacent embryonic, vegetative, and floral organs. Current Biology **14**, 1035–1046.

Marin E, Jouannet V, Herz A, Lokerse AS, Weijers D, Vaucheret H, Nussaume L, Crespi MD, Maizel A. 2010. miR390, *Arabidopsis TAS3* tasiRNAs, and their *AUXIN RESPONSE FACTOR* targets define an autoregulatory network quantitatively regulating lateral root growth. The Plant Cell **22**, 1104–1117.

Mason MG, Li J, Mathews DE, Kieber JJ, Schaller GE. 2004. Type-B response regulators display overlapping expression patterns in Arabidopsis. Plant Physiology **135**, 927–937.

Morea EG, da Silva EM, e Silva GF, Valente GT, Barrera Rojas CH, Vincentz M, Nogueira FT. 2016. Functional and evolutionary analyses of the miR156 and miR529 families in land plants. BMC Plant Biology **16**, 40.

Motte H, Vereecke D, Geelen D, Werbrouck S. 2014. The molecular path to *in vitro* shoot regeneration. Biotechnology Advances **32**, 107–121.

Müller B, Sheen J. 2008. Cytokinin and auxin interaction in root stem-cell specification during early embryogenesis. Nature **453**, 1094–1097.

Murashige T, Skoog F. 1962. A revised medium for rapid growth and bio assays with tobacco tissue cultures. Physiologia Plantarum **15**, 473–497.

Nodine MD, Bartel DP. 2010. MicroRNAs prevent precocious gene expression and enable pattern formation during plant embryogenesis. Genes & Development **24**, 2678–2692.

Osmont KS, Sibout R, Hardtke CS. 2007. Hidden branches: developments in root system architecture. Annual Review of Plant Biology **58**, 93–113.

Péret B, De Rybel B, Casimiro I, Benková E, Swarup R, Laplaze L, Beeckman T, Bennett MJ. 2009. *Arabidopsis* lateral root development: an emerging story. Trends in Plant Science **14**, 399–408.

Pernisova M, Grochova M, Konecny T, Plackova L, Harustiakova D, Kakimoto T, Heisler MG, Novak O, Hejatko J. 2018. Cytokinin signalling regulates organ identity via the AHK4 receptor in *Arabidopsis*. Development **145**, dev163907.

Petersson SV, Johansson AI, Kowalczyk M, Makoveychuk A, Wang JY, Moritz T, Grebe M, Benfey PN, Sandberg G, Ljung K. 2009. An auxin gradient and maximum in the *Arabidopsis* root apex shown by high-resolution cell-specific analysis of IAA distribution and synthesis. The Plant Cell **21**, 1659–1668.

Qiao M, Zhao Z, Song Y, Liu Z, Cao L, Yu Y, Li S, Xiang F. 2012. Proper regeneration from *in vitro* cultured *Arabidopsis thaliana* requires the microRNA-directed action of an auxin response factor. The Plant Journal **71**, 14–22.

Rodriguez RE, Ercoli MF, Debernardi JM, Breakfield NW, Mecchia MA, Sabatini M, Cools T, De Veylder L, Benfey PN, Palatnik JF. 2015. MicroRNA miR396 regulates the switch between stem cells and transit-amplifying cells in *Arabidopsis* roots. The Plant Cell **27**, 3354–3366.

Rubio-Somoza I, Weigel D. 2011. MicroRNA networks and developmental plasticity in plants. Trends in Plant Science **16**, 258–264.

Sakai H, Honma T, Aoyama T, Sato S, Kato T, Tabata S, Oka A. 2001. ARR1, a transcription factor for genes immediately responsive to cytokinins. Science **294**, 1519–1521.

Sakai WS. 1973. Simple method for differential staining of paraffin embedded plant material using toluidine blue o. Stain Technology **48**, 247–249.

Schwarz S, Grande AV, Bujdoso N, Saedler H, Huijser P. 2008. The microRNA regulated SBP-box genes *SPL9* and *SPL15* control shoot maturation in *Arabidopsis*. Plant Molecular Biology **67**, 183–195.

Senecoff JF, McKinney EC, Meagher RB. 1996. *De novo* purine synthesis in *Arabidopsis thaliana*. II. The *PUR7* gene encoding 5'-phosphoribosyl-4-(N-succinocarboxamide)-5-aminoimidazole synthetase is expressed in rapidly dividing tissues. Plant Physiology **112**, 905–917.

Silva GFF, Silva EM, Correa JPO, *et al*. 2019. Tomato floral induction and flower development are orchestrated by the interplay between gibberellin and two unrelated microRNA-controlled modules. New Phytologist **221**, 1328–1344.

Silva GFF, Silva EM, Silva M, *et al*. 2014. microRNA156-targeted SPL/SBP box transcription factors regulate tomato ovary and fruit development. The Plant Journal **78**, 604–618.

Skoog F, Miller CO. 1957. Chemical regulation of growth and organ formation in plant tissues cultured *in vitro*. Symposia of the Society for Experimental Biology **11**, 118–130.

Su YH, Zhang XS. 2009. Auxin gradients trigger *de novo* formation of stem cells during somatic embryogenesis. Plant Signaling & Behavior **4**, 574–576.

Sugimoto K, Jiao Y, Meyerowitz EM. 2010. Arabidopsis regeneration from multiple tissues occurs via a root development pathway. Developmental Cell **18**, 463–471.

Takatsuka H, Umeda M. 2014. Hormonal control of cell division and elongation along differentiation trajectories in roots. Journal of Experimental Botany **65**, 2633–2643.

Ubeda-Tomás S, Swarup R, Coates J, Swarup K, Laplaze L, Beemster GT, Hedden P, Bhalerao R, Bennett MJ. 2008. Root growth in Arabidopsis requires gibberellin/DELLA signalling in the endodermis. Nature Cell Biology **10**, 625–628.

Ulmasov T, Murfett J, Hagen G, Guilfoyle TJ. 1997. Aux/IAA proteins repress expression of reporter genes containing natural and highly active synthetic auxin response elements. The Plan Cell **9**, 1963–1971.

Usami T, Horiguchi G, Yano S, Tsukaya H. 2009. The *more and smaller cells* mutants of *Arabidopsis thaliana* identify novel roles for *SQUAMOSA PROMOTER BINDING PROTEIN-LIKE* genes in the control of heteroblasty. Development **136**, 955–964.

Valvekens D, Van Montagu M, Van Lijsebettens M. 1988. *Agrobacterium tumefaciens*-mediated transformation of *Arabidopsis thaliana* root explants by using kanamycin selection. Proceedings of the National Academy of Sciences, USA **85**, 5536–5540.

Varkonyi-Gasic E, Wu R, Wood M, Walton EF, Hellens RP. 2007. Protocol: a highly sensitive RT-PCR method for detection and quantification of microRNAs. Plant Methods **3**, 12.

Vieten A, Vanneste S, Wisniewska J, Benková E, Benjamins R, Beeckman T, Luschnig C, Friml J. 2005. Functional redundancy of PIN proteins is accompanied by auxin-dependent cross-regulation of PIN expression. Development **132**, 4521–4531.

Wang JW, Schwab R, Czech B, Mica E, Weigel D. 2008. Dual effects of miR156-targeted *SPL* genes and *CYP78A5/KLUH* on plastochron length and organ size in *Arabidopsis thaliana*. The Plant Cell **20**, 1231–1243.

Wang JW, Wang LJ, Mao YB, Cai WJ, Xue HW, Chen XY. 2005. Control of root cap formation by microRNA-targeted auxin response factors in *Arabidopsis*. The Plant Cell **17**, 2204–2216.

Wisniewska J, Xu J, Seifertová D, Brewer PB, Ruzicka K, Blilou I, Rouquié D, Benková E, Scheres B, Friml J. 2006. Polar PIN localization directs auxin flow in plants. Science **312**, 883.

Wu G, Poethig RS. 2006. Temporal regulation of shoot development in *Arabidopsis thaliana* by *miR156* and its target *SPL3*. Development **133**, 3539–3547.

Wu G, Park MY, Conway SR, Wang JW, Weigel D, Poethig RS. 2009. The sequential action of miR156 and miR172 regulates developmental timing in Arabidopsis. Cell **138**, 750–759.

Xie K, Shen J, Hou X, Yao J, Li X, Xiao J, Xiong L. 2012. Gradual increase of miR156 regulates temporal expression changes of numerous genes during leaf development in rice. Plant Physiology **158**, 1382–1394.

Xu M, Hu T, Zhao J, Park MY, Earley KW, Wu G, Yang L, Poethig RS. 2016. Developmental functions of miR156-regulated *SQUAMOSA PROMOTER BINDING PROTEIN-LIKE* (*SPL*) genes in *Arabidopsis thaliana*. PLoS Genetics **12**, e1006263.

Xu M, Leichty AR, Hu T, Scott Poethig R. 2018. H2A.Z promotes the transcription of *MIR156A* and *MIR156C* in Arabidopsis by facilitating the deposition of h3k4me3. Development **145**, dev152868.

Xu X, Li X, Hu X, Wu T, Wang Y, Xu X, Zhang X, Han Z. 2017. High miR156 expression is required for auxin-induced adventitious root formation

via *MxSPL26* independent of *PINs* and *ARFs* in *Malus xiaojinensis*. Frontiers in Plant Science **8**, 1059.

Yang L, Xu M, Koo Y, He J, Poethig RS. 2013. Sugar promotes vegetative phase change in *Arabidopsis thaliana* by repressing the expression of *MIR156A* and *MIR156C*. eLIFE **2**, e00260.

Yoon EK, Yang JH, Lim J, Kim SH, Kim SK, Lee WS. 2010. Auxin regulation of the microRNA390-dependent transacting small interfering RNA pathway in *Arabidopsis* lateral root development. Nucleic Acids Research **38**, 1382–1391.

Yu N, Cai WJ, Wang S, Shan CM, Wang LJ, Chen XY. 2010. Temporal control of trichome distribution by microRNA156-targeted *SPL* genes in *Arabidopsis thaliana*. The Plant Cell **22**, 2322–2335.

Yu N, Niu QW, Ng KH, Chua NH. 2015. The role of miR156/SPLs modules in *Arabidopsis* lateral root development. The Plant Journal **83**, 673–685.

Zhang TQ, Lian H, Tang H, *et al*. 2015. An intrinsic microRNA timer regulates progressive decline in shoot regenerative capacity in plants. The Plant Cell **27**, 349–360.

Zobel RW. 1986. Rhizogenetics (root genetics) of vegetable crops. HortScience **21**, 956–959.

Zürcher E, Tavor-Deslex D, Lituiev D, Enkerli K, Tarr PT, Müller B. 2013. A robust and sensitive synthetic sensor to monitor the transcriptional output of the cytokinin signaling network *in planta*. Plant Physiology **161**, 1066–1075.